ESTIMATION OF CLEAR-WATER LOCAL SCOUR AT PILE GROUPS USING GENETIC EXPRESSION PROGRAMMING (GEP) AND MULTIVARIATE ADAPTIVE REGRESSION SPLINES (MARS)

A THESIS SUBMITTED TO THE GRADUATE DIVISION OF THE UNIVERSITY OF HAWAIʻI AT MĀNOA IN PARTIAL FULFILLMENT OF THE REQUIREMENTS FOR THE DEGREE OF:

MASTER OF SCIENCE

IN

CIVIL ENGINEERING

SEPTEMBER 2017

By

Bryan A. Truce

Thesis Committee:

Sayed M. Bateni, Chairperson

Roger W. Babcock, Jr.

Oceana P. Francis

ACKNOWLEDGMENTS

I would like to acknowledge and thank the people who have helped me on my path to completing this thesis. First, I would like to thank my advisor Sayed Bateni, for bringing me out to the University of Hawaii and taking me on as a Research Assistant, along with finding me a place to live and work, along with aiding him as a Teaching Assistant in the field of Fluid Mechanics. I would also like to thank the other two members of the committee, Roger Babcock Jr. and Oceana Francis, who justified my research by evaluating my defense.

I would like to thank Dr. Behzad Ataie-Ashtiani, from the Department of Civil Engineering at the Sharif University of Technology. Dr. Behzad Ataie-Ashtiani was invaluable in his commitment to the topic of pile scour and his efforts of collaboration in bringing together the data from over 16 different sources from all around the world. Also, I would like to express my special thanks to Emily Stack who I have worked with on Gene Expression Programming.

Lastly, I would like to express my special thanks to Katrina Linegar who moved from her home in the mainland to Hawaii and be here for me all along the way. I would also like to thank my brother, mother, and father for supporting, encouraging, and inspiring me.

ABSTRACT

The physical process of scour around pile groups is complex. Due to economical and geotechnical reasons, group piles have become more common in bridge designs. Various empirical models have been developed to estimate maximum scour depth at pile groups. However, these models are mostly based on the conventional statistical regression approaches, and are not able to adequately capture the highly nonlinear and complex relationship between scour depth and its influential factors. In this study, Multivariate Adaptive Regression Splines (MARS) and Genetic Expression Programming (GEP) were used to estimate clear-water local scour depth at pile groups from the current, sediment, and pile characteristics. Two combinations of data were used to train the GEP and MARS models. The first combination includes mean flow velocity, flow depth, mean grain diameter, pile diameter, distance between the piles, and the number of piles normal to the flow and in-line with the flow. The second combination contains seven non-dimensional parameters. Results indicated that MARS and GEP can generate accurate scour depth estimates. Both models yield better results when the dimensional data were used. Also, it was found that the MARS model (with root-mean-square-error (RMSE) of 0.0110 m and correlation coefficient (R^2) of 0.969 outperformed the GEP model (with RMSE of 0.0187 m and R^2 of 0.911). The performance of GEP and MARS models was compared with that of the existing empirical methods. The comparison showed that both models perform better than the regression-based empirical equations. Finally, a sensitivity analysis showed that the pile diameter in dimensional combination and ratio of pile spacing to pile diameter in non-dimensional combination have the most significant impact on scour depth.

Contents

LIST OF TABLES

LIST OF FIGURES

1. Introduction

1.1. Background

When a stream is partially obstructed by a bridge pier, the flow pattern around the pier is changed (**Figure 1**). The pier produces an adverse pressure gradient just upstream of the pier, and a corresponding uplift pressure that lifts the sediment from the bed surface. The boundary layer upstream of the pier undergoes a three-dimensional separation and the shear stress distribution around the pier is drastically changed. This is due to the formation of a horseshoe vortex, which results in the formation of a scour hole around the pier (**Figure 1**) and changes the flow pattern and shear (Kothyarie et al., 1992).

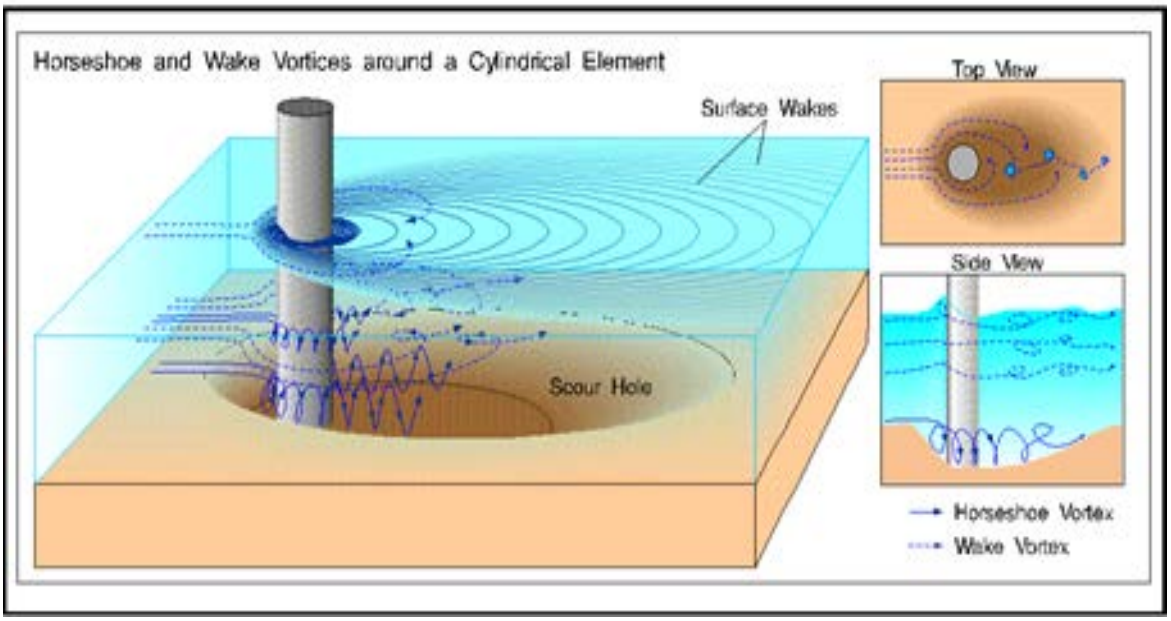

Figure 1. The scour hole around the bridge pier (Hill, 2013)

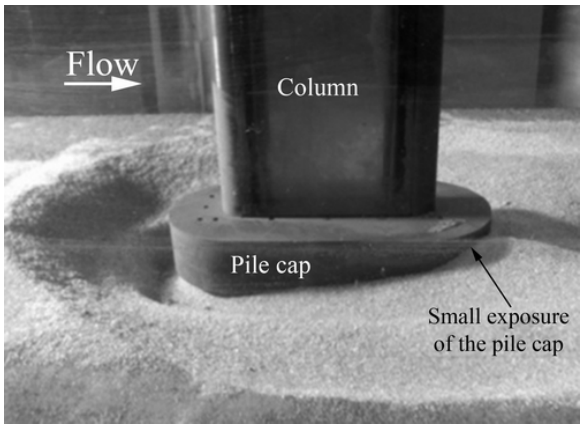

Figure 2. Examples of scour depth around piles: (top) adopted from Ferraro et al. (2013), (middle) scour hole at the New Independencia Bridge on Piura River (Vasquez, 2004), and (Bottom) taken from the Leader-Herald (2017).

As shown in top two images in **Figure 2**, local scour around bridge foundations leads to degradation around the pile, which weakens the structural support of the pile, eventually leading to the collapse of bridge piers and decks (Moreno et al., 2015), as shown in the bottom image of **Figure 2**. Wardhana and Hadipriono (2003) studied over 500 bridge failures in the United States, between 1989 and 2000. The average age of the failed bridges was about 52.5 years. The main cause of bridge failures was due to flooding. Scour due to flood contributed to nearly 53% of all failures (Wardhana and Hadipriono, 2003).

Piles groups provide an efficient use of footprints for the foundation of bridges. They provide us with the ability to provide the maximum amount of load over the minimum amount of footprint area. This is done with the use of an elongated side friction surface area. However, when that elongated side friction surface area changes due to the effects of climate change and natural erosion, the efficient use of footprint may become susceptible to failure.

As stated by Coleman (2005), "physical and economic considerations often lead to bridge foundations being constructed of a pile or pile group". For geotechnical and economic reasons, multiple piles have become more and more popular in bridge design (Ataie-Ashtiani and Beheshti, 2006). These studies demonstrated that group of piles can significantly reduce construction costs compared to those spread footer structures, especially when sediment scour is a consideration. As stated, this type of support structure (that of a pile) can be eroded as well, and understanding that erosion (or scour) is the goal of this study.

Pile groups are widely used to support marine structures in coastal areas and bridges on deep alluvial riverbeds. These types of alluvial beds typically have fine sediments from the erosion of the surrounding hillsides or mountains. These fine sediments are more susceptible to uplift pressure around piles. Climate change causes more extreme weather and flooding conditions. Due

to the climate change and rising flood level, pile caps and other parts of the foundations of a bridge pile may become submerged and develop characteristics of submerged piles (Amini et al., 2012), which are subjected to a higher flow velocity. This can accelerate the scour process.

In major river crossings, there is an increasing use of bridge foundations that consist of a number of piles supporting a pile cap. Piers composed of columns and a pile cap are also known as complex piers. These types of foundations of the piles are often deep. However, if these types of piles rely on the skin friction (the friction caused between the pile and the surrounding soil) rather than the end-loading (pile load supported primarily by the end of the pile) to support the weight of the bridge, the foundation can be more vulnerable to scour. The focus of this paper will be solely on piles. All research data was cleaned to eliminate the effects of a pile cap.

An accurate estimation of scour depth around piles is required for a safe and economic design of bridges and harbors (Etemad-Shahidi et al., 2011). However, scour is a complex phenomenon that is affected by many variables. Besides the physical variables (e.g., pier geometry, flow velocity, and sediment characteristics), there are several non-physical processes (e.g., turbulent boundary layer, time-dependent flow pattern and sediment transport mechanism) that can all affect the scour mechanism. These combined physical and non-physical factors make the prediction of scour depth challenging. Hence, even though many experimental and theoretical studies have been conducted to predict scour depth around bridge piers, there is still a need for further improvement in the existing empirical relations.

1.2. Influential Variables

Scour depth around piers has been estimated by many studies (Dey and Barbhuya, 2004a and b, Ataie-Ashtiani et al, 2010, Azamathulla, 2012, Cheng and Cao, 2014, and Choi et. al., 2015). These studies have led to various empirical formulas to relate the scour depth to its influential variables. These input variables are the key to the prediction of scour depth. The variables associated with the flow properties, sediment characteristics and pile geometry are found in almost all empirical formulas that predict the scour depth.

Richardson and Davis (2001) evaluated the effect of flow velocity and pier diameter on the pile scour depth. They found that the scour depth has a direct correlation with flow velocity, i.e., the greater the velocity, the deeper the scour depth. Flow depth also has a direct correlation with the scour depth. An increase in flow depth can increase scour depth by a factor of 2 or more. Pier diameter was also found to be a significant factor. As pier diameter increases, there is an increase in scour depth. However, there is a limit for this increase. Very wide piers do not have scour depths as deep as predicted by existing formulas.

Equation 1 represents the relationship between the scour depth (d_{se}) and its influential variables (Amini et al., 2012):

$$d_{se} = f_1(\rho, \mu, g, D, y, U, U_c, d_{50}, S_m, S_n, n, m) \quad (1)$$

where μ is the fluid dynamic viscosity, ρ is the fluid density, U is the flow mean velocity, U_c is the critical flow velocity associated with the start of motion of particles on the bed surface, y is the flow depth, g is the gravitational acceleration, D is the pile diameter, and d_{50} is the sediment mean diameter, n is the number of piles normal to the flow, m is the number of piles in line with the flow, S_n is the spacing between piles normal to the flow, S_m is the spacing between piles in line

with the flow, and d_{se} is the scour depth around pile group (**Figure 3**). By using the dimensional analysis, the twelve independent variables can be decreased to a set of eight non-dimensional parameters as follows,

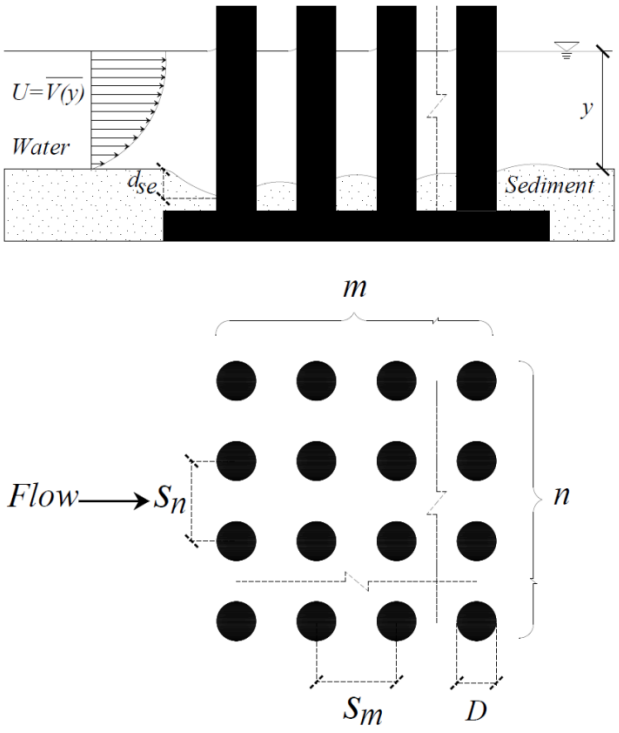

Figure 3. Schematic of variables involved in the prediction of scour.

$$\frac{dse}{D} = f_2\left(\frac{U}{U_c}, \frac{U^2}{gD}, \frac{y}{D}, \frac{D}{d_{50}}, \frac{\rho UD}{\mu}, \frac{S_m}{D}, \frac{S_n}{D}, \frac{m}{n}\right) \quad (2)$$

Equation 2, (Amini et al., 2012) shows how the various physical processes such as fluid-structure interaction, fluid-seabed interaction, and sediment transport affect the scour mechanism. The Reynolds number ($\frac{\rho UD}{\mu}$), the square of the Froude number ($\frac{U^2}{gD}$), and depth to diameter ratio account for the flow characteristics around the piles. U/U_c describes the influence of flow on the

seabed and D/d_{50} indicates the interaction between pile and bed sediment (Etemad-Shahidi et al., 2011)

1.3. Challenges in Scour Prediction

Lack of understanding of the complex scour processes and their simplified modeling have led to a pronounced uncertainty in predicting the scour depth (Azamathulla, 2012). This is mainly because 1) the exact mechanism of scour and effects of different parameters on scour depth are not yet fully understood (Dey and Barbhuya, 2004 a, b), and 2) the conventional regression-based approaches cannot accurately capture effects of influential parameters on scour depth (Ettema et al, 1998).

The regression-based relationships are used commonly to predict scour depth at bridge abutments. However, these expressions typically lead to large uncertainties. This can have major drawbacks pertaining to the idealization of the complex scour processes. This combined with a lack of reliable data leads to an inaccuracy in the estimation of scour depth. Therefore, empirical regression-based equations typically overestimate the scour depth and generate conservative results (US DOT, 1993; Ettema et al, 1998; Melville and Chew, 1999).

Although many studies (e.g., US DOT, 1993; Coleman, 2005; Ataie-Ashtiani et al., 2010; Toth and Brandiarte, 2011; Azamathulla, 2012; Choi et al., 2015; Toth, 2015) have been carried out in this field, there is a lack of reliable formulas for prediction of scour depth. The results from the existing methods highly differ with each other, thus resulting in big controversy in design and cost of the protection methods against scour and the foundations of the piers (Ettema et al., 1998). Moreover, each empirical formula may work well for a specific data set, but many fall short when applied to similar data sets, with slightly different variables. This becomes increasingly important

for piers that may be termed wide by virtue of their large diameter, or width, relative to flow depth. For increasingly wide piers, greater accuracy is needed because the cost of conservation becomes inordinately large for such designs (Bateni et al, 2007).

1.4. Alternative Methods to the Regression-Based Approaches

1.4.1. Artificial Neural Networks (ANN)

Recognizing the shortcomings of regression-based equations and the importance of improving prediction capabilities, a number of studies have used the Artificial Neural Network (ANN) approach to estimate scour depth around piles (Choi and Jung, 2006; Bateni et al., 2007a, b; Kaya, 2010; Toth and Brandimarte, 2011; Choi et al., 2015; Toth, 2015).

Regression-based formulas tend to give conservative estimates of scour depth around bridge piers, while the more advanced ANN gives more accurate predictions. This is because the complexity of the physical processes involved in the scour problem, can be captured more robustly by the ANN (Zhang and Goh, 2013). However, the ANN approach is often not as readily available as the empirical formulas. Nonetheless, with the rapid increases in processing speed and memory of low-cost computers, ANN has been used for modeling highly nonlinear, multivariate engineering problems (Zhang and Goh, 2013). During the last two decades, many studies (e.g., Samui, 2011, Azamthulla, 2012, Emamgholizadeh et al., 2015) showed that the soft computing techniques such as ANN, GEP, and MARS yielded better results that the conventional statistical methods. ANN has been used as an alternative method to capture complexity in physical modeling. In recent years, this approach has become an effective tool for providing hydraulic and environmental engineers with more accuracy for design purposes and management practices (Bateni et al., 2007a). A typical configuration of an ANN model is shown in **Figure 4.** Structure of a typical ANN model (Bateni et al., 2007).. A set of data is first fed directly in the ANN model

through the input layer. Then ANN produces an expected result, y, in the output layer. The number of hidden layers establishes the complexity of the network because a greater number of hidden layers increases the number of connections in the ANN.

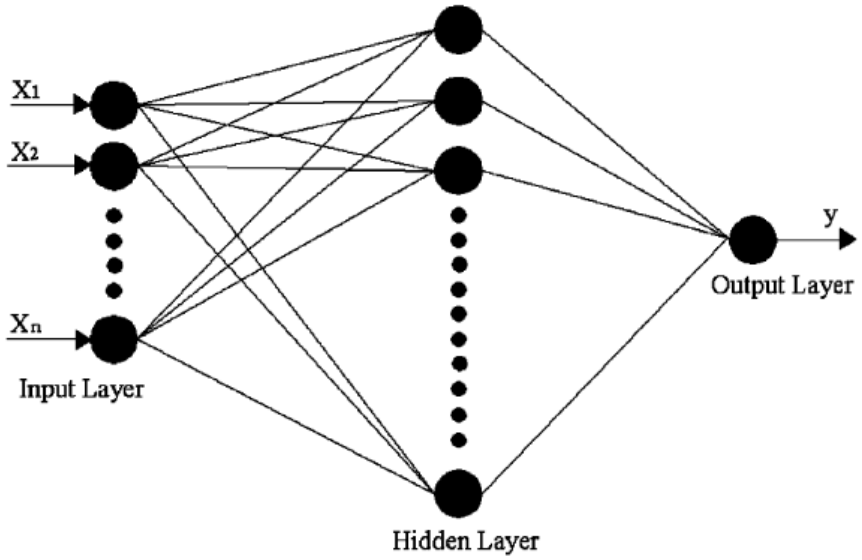

Figure 4. Structure of a typical ANN model (Bateni et al., 2007).

The number of hidden layers and nodes in each hidden layer are found by trial and error. Each node multiplies its corresponding input by its interconnection weight, sums the product, and then passes the sum through a transfer function to produce the result. This transfer function is usually a steadily increasing S-shape curve called a sigmoid function. Under this threshold function the output, y_j, for the *j*th neuron in a layer is:

$$y_j = f(\sum w_{ij} x_i) = \frac{1}{1+e^{-(\sum w_{ij} x_i)}} \quad (3)$$

where w_{ij} is the weight of the connection joining the *j*th neuron in a layer to the *i*th neuron in the previous layer and x_i is the value of the *i*th neuron in the previous layer.

The ANN is trained with a set of known input and output data. Many learning examples are repeatedly presented to the network, and the process is terminated when the number of training iterations excesses a specified value. At this stage, ANN is considered as trained (Bateni et al., 2007).

1.4.2. Gene Expression Programming (GEP) and Multi-Adaptive Regression Spines (MARS)

Despite the outperformance of ANN models over the regression-based approaches, they operate as a black-box and cannot provide an explicit equation between the scour depth and its influential variables. Because of shortcomings of regression-based and ANN methods, this study used Genetic Express Programming (GEP) and Multivariate Adaptive Regression Splines (MARS) to estimate scour depth around piles.

GEP was developed by Ferreira (2001 a, b). It is an optimization method that can robustly simulate the complex relationship between a dependent variable and its influential factors. MARS is a non-parametric model that was developed by Friedman (1991). To the best of our knowledge, GEP and MARS have not been used in other studies to estimate scour depth around pile groups.

GEP and MARS do not suffer from the abovementioned shortcomings of the regression-based and ANN approaches and have several advantages: (1) they can generate an explicit relationship between the response variable and its predictors, (2) they do not perform like a black-box, (3) they can simulate the complicated relationship between the dependent variable and its influential independent variables, (4) they do not require to presume *a priori*, specific form of function to relate inputs to output(s), and (5) they are more flexible than the regression methods and typically can overcome their limitations (Samui et al., 2011; Gandomi and Alavi, 2011; Zhang and Goh, 2013).

GEP and MARS have been used by several studies (e.g., Guven and Aytek, 2009; Azamathulla, 2012; Adamowski et al., 2012; Sattar, 2014; Cheng and Cao, 2014) and in many engineering problems to capture complicated relationships between inputs and outputs. Shiri et al. (2012) used GEP to estimate daily evaporation. Guven and Azamathulla (2012) compared MARS with ANN for runoff forecasting in the mountainous watershed of Sainji in the Himalays, and found their performance is comparable. Emamgholizadeh et al. (2015) used MARS and GEP to estimate the soil cation exchange capacity from its easily measurable variables. Samui (2011) utilized MARS to predict the ultimate capacity of piles in cohesionless soils. GEP and ANN were used by Kisi and Shiri (2012) to evaluate the suspended sediment concentration in the Eel River. GEP was used successfully in hydraulic engineering problems: estimation of scour depth downstream of hydraulic structures (Guven and Gunal, 2008) and scour depth downstream of naturally occurring structural sill (Azamathulla, 2012), dispersion coefficients in natural streams and pipes (Azamathulla and Wu, 2011), dam breach parameters (Sattar, 2014), and effective transverse mixing of fluids (Azamathulla and Ahmand, 2012). These studies showed that GEP and MARS performed better than ANN. In fact, the above studies (among many others) showed that outcomes of GEP and MARS have better predictability than those of commonly used empirical approaches in most engineering problems.

Another complexity is how the piles behave in a fluid, not only as an individual pile, but grouped together. Local scour at pile groups is more complex and difficult to predict than that at single piles. The increased complexity is due to the interaction of vortices generated at the individual piles and the interdependence of scour holes around each pile (Lanca et al., 2013). As discussed, piles are often built in areas with currents such as harbor and waterfronts. Although scour around “single piles” has been widely studied by many researchers, a limited number of

studies have been conducted on scour around “pile groups”. In contrast to other types of footings, pile group foundations are considered significantly cost-effective, regarding the influence of scour phenomenon (Etemad-Shahidi et al., 2011). In order to study the effects of pile scour amongst group an alternative dimensionless form of equilibrium scour can also be analyzed.

The first goal of this study is to develop and test GEP- and MARS-based equations for the prediction of scour depth around pile groups. Our second objective is to compare scour depth estimates from GEP and MARS. Finally, performance of GEP and MARS is compared with the existing regression-based equations. In this study, we consider the variables that have been used in the literature to predict scour around pile groups.

2. Data

2.1. Sources of Data

In this study, data were obtained from various experimental studies. These experiments were generally conducted in a flume with an adjustable inflow rate (**Figure 5**). Different configurations of piles groups were used in the experiments in the flume. Different experiments were conducted by changing the inflow rate, number and configuration of piles within the pile group, and sediment size. As shown in Figure 8, there is an intake of water at point 1 that is connected to the pump in point 2. The water is conveyed to the flume in point 3. At position 4, there is a screen to decrease the water-surface fluctuations. Thereafter, the water flows over coarse sediments in zones 5 and 6 to reduce its turbulence, and finally flows over the fine sediments and pile configuration in positions 7 and 8. The water flows out of the flume in point 9.

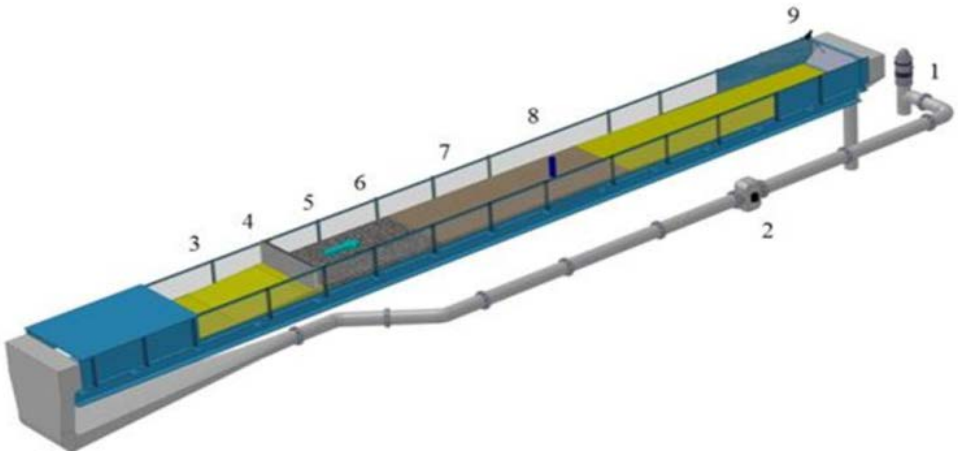

Figure 5. General set up for an experimental flume.

A total of 269 experimental data points from 16 studies were used in this study. The first study was conducted by Ataie-Ashtiani et al. (2010). They investigated the local scour around compound piers. Their experiments were carried out in a 4.0 (m) long, 0.6 (m) wide and 0.3 (m) deep flume at the Sharif University of Technology, in Iran. Their study used complex pier

geometry. The complex pier geometry refers to piles, which are covered by a pile cap. The pile cap can alter the flow condition around the pile. Since this study focuses only on piers and piles, all data that involve the pile cap were not used. The water surface can be above, in line with or below the pile cap. In this study, only experiments in which the water level is below the pile cap were included. This was done to eliminate the effect of the pile cap on the scour depth.

The second study was performed by Coleman (2005). He investigated the scour process at complex piers by exposing them to five different water level scenarios. The experiments were run in two different facilities, one in New Zealand and the other one in the United States. In both of the facilities, the tests were performed in a 43 m long and 1.5 m wide, glass-sided flume.

In the third study, conducted by Ferraro et al. (2013), the effect of pile cap thickness on the temporal evolution of the scour depth and the equilibrium scour was evaluated. Each test lasted for a duration longer than the equilibrium time suggested by Colman (2005). The experiments were performed in an 8 m long, 0.70 m wide, and 0.70 m deep glass-walled horizontal flume. Various experiments with different pile cap thicknesses, distances between the pile caps, and the initial bed levels (Y) were implemented. Y is positive when the pile cap is above the water level. Therefore, no negative values of Y were used.

The fourth study was conducted by Grimaldi and Cardoso (2010). They evaluated seven different complex piers configurations, all with various water levels above and below the pier cap. As mentioned above, in this study, only the experiments in which the pile cap is entirely above the water surface are considered. Experiments were done in a flume, which is made of steel with glass side walls. The flume length and width were 8.0 (m) and 0.7 (m), respectively.

In the fifth study, performed by Moreno et al. (2014), they ran the experiment in 8 flumes for scouring at complex piers. The aim of this study was to evaluate the contribution of complex

pier components on the scour depth. Their study presented a new approach to estimate the scour depth by taking into account different components of complex piers.

In another study conducted by Moreno et al. (2015), the effect of relative column width and pile-cap elevation on scour depth around complex piers was investigated. Their experiments were carried out in the National Laboratory for Civil Engineering (LNCE) in Lisbon, in a glass sided rectangular flume with a length of 40 m, width of 2.0 m, and depth of 1.0 m. In their study, 11 pile cap positions relative to the water surface level were analyzed and labeled as positions A-K. These 11 positions were associated with three cases. In case 1 (positions A-D), the pile cap was above the water surface level. In case 2 (positions E-H), the pile cap was partially in the flowing water, and finally in case 3 (positions I-K), the pile cap was completely under the water surface. In this project, only the experimental data from case 1 were used where the pile cap was above the water surface.

The seventh study was carried out by Martin-Vide et al. (1998). They investigated the local scour at piles. In their study, a total of 27 interface elevations (height of water level with respect to the pile cap) were tested under the same flow conditions. These experiments were conducted in a 5.80 m long and 1.50 m wide flume.

In the eighth study, Ataie and Beheshti (2006) investigated the local scour around a group of piles and compared performance of the commonly used formulas. Their experiments were carried out in a 4 m long, 0.41 m wide, and 0.25 m deep flume.

In the ninth study, Amini et al. (2012) investigated the clear-water scour at pile groups. In their study, a wide range of pile group arrangements, and spacing were examined. Their experiments were conducted in 46 m length, 1.52 m width and 1.9 m flume. They concluded that

local scour depends on pile diameter, and pile spacing, and proposed a new empirical method to estimate local scour depth at the pile groups.

The tenth study was performed by Sheppard (2003). His study proposed a methodology to estimate local scour depth at a group of piles.

2.2. Pile Scour Laboratory Data

Scour depth data were obtained from six other studies (Hajzaman, 2008, Moreno et al., 2014, Oliveto et al., 2004, Hannah, 1978, Zhao and Sheppard, 1998, and Lanca et al., 2013). The above-mentioned 16 studies are listed in **Table 1**. The utilized data are shown in **Table 2**. The measured variables include the scour depth (d_{se}), average particle diameter size (d_{50}), flow depth (y), and mean flow velocity (U) and the critical flow velocity (U_c). Physical characteristics of the piles (i.e., pile diameter (D), the number of piles parallel (m) and perpendicular (n) to flow, and the distance of piles from each other parallel (S_m) and perpendicular to flow (S_n)) were also included in these data sets. The range of different variables used in this study is presented in **Table 3**. The data was separated randomly and 80% of the data was used to train the MARS and GEP models and 20% of the data was used to test the validity of the models.

Table 1. List of studies that were used in this research.

	Studies	Lab
1	Ataie-Ashtiani et al. (2010)	Sharif University of Technology, Tehran
2	Hajzaman (2008)	Sharif University of Technology, Tehran
3	Coleman (2005)	University of Aukland, New Zealand
4	Ferraro et al. (2013)	Instituto Superior Técnico, Portugal
5	Cardoso (2010)	Instituto Superior Tecnico, Lisbon, Portugal
6	Moreno et al. (2014)	Instituto Superior Tecnico, Lisbon, Portugal
7	Moreno et al. (2014)	Canal de Inclinação Variável (CIV)
8	Moreno et al. (2015)	National Laboratory for Civil Engineering, Lisbon, Portugal
9	Oliveto et al. (2004)	University of Basilicata
10	Martin-Vide et al. (1998)	Civil Engineering School, Barcelona, Spain
11	Ataie and Beheshti (2006)	Sharif University of Technology, Tehran
12	Lanca et al. (2013)	Dept. de Engenharia Civil, Instituto Superior, Faro, Portugal
13	Amini et al. (2012)	Hydraulic Laboratory of Malaysia (NAHRIM)
14	Hannah (1978)	Civil Engineering Department, University of Canterbury, Christchurch, New Zealand
15	Sheppard (1998)	Hydraulics Laboratory, University of Florida
16	Sheppard (2003)	Conte USGS Laboratory, University of Florida

Table 2. Data points of the 16 studies in Table 1.

	Reference	d_{se} (m)	d_{50} (mm)	y (m)	U (m/s)	U_c (m/s)	D (m)	m	n	S_m (m)	S_n (m)
1	**1**	0.048	0.6	0.144	0.234	0.31	0.016	3	2	0.040	0.032
2	**1**	0.053	0.6	0.142	0.237	0.31	0.016	3	2	0.040	0.032
3	**1**	0.038	0.6	0.140	0.262	0.34	0.016	3	2	0.065	0.048
4	**2**	0.058	0.6	0.127	0.230	0.31	0.022	3	2	0.045	0.03
5	**2**	0.066	0.6	0.130	0.228	0.31	0.022	3	2	0.045	0.03
6	**2**	0.039	0.6	0.143	0.228	0.32	0.016	3	2	0.045	0.03
7	**2**	0.047	0.6	0.143	0.227	0.32	0.016	3	2	0.045	0.03
8	**2**	0.039	0.6	0.145	0.230	0.32	0.016	4	2	0.036	0.03
9	**2**	0.037	0.6	0.139	0.230	0.32	0.016	4	2	0.036	0.03
10	**2**	0.066	0.6	0.142	0.234	0.32	0.022	4	2	0.036	0.03
11	**2**	0.052	0.6	0.139	0.236	0.32	0.022	4	2	0.036	0.03
12	**3**	0.125	0.84	0.330	0.340	0.41	0.02	8	3	0.060	0.065
13	**3**	0.077	0.84	0.600	0.375	0.44	0.024	4	2	0.072	0.072
14	**3**	0.068	0.84	0.600	0.330	0.44	0.024	4	2	0.072	0.072
15	**4**	0.101	0.83	0.100	0.271	0.30	0.025	5	2	0.050	0.055
16	**5**	0.096	0.83	0.100	0.290	0.29	0.025	2	2	0.075	0.075
17	**6**	0.135	0.86	0.180	0.310	0.32	0.05	4	1	0.125	0
18	**7**	0.114	0.86	0.200	0.258	0.32	0.05	4	2	0.125	0.125
19	**8**	0.123	0.86	0.200	0.258	0.32	0.05	4	2	0.125	0.125
20	**8**	0.123	0.86	0.200	0.258	0.32	0.05	4	2	0.125	0.125
21	**8**	0.123	0.86	0.200	0.258	0.32	0.05	4	2	0.125	0.125
22	**9**	0.058	2.4	0.114	0.433	0.53	0.02	2	2	0.020	0.02
23	**9**	0.029	2.4	0.114	0.433	0.53	0.02	2	2	0.040	0.04
24	**9**	0.022	2.4	0.114	0.433	0.53	0.02	2	2	0.060	0.06
25	**9**	0.025	2.4	0.114	0.433	0.53	0.02	2	2	0.080	0.08
26	**9**	0.021	2.4	0.114	0.433	0.53	0.02	2	2	0.100	0.1
27	**10**	0.093	0.65	0.254	0.326	0.35	0.06	2	1	0.240	0
28	**11**	0.029	0.98	0.033	0.246	0.31	0.016	1	1	0	0
29	**11**	0.028	0.98	0.035	0.232	0.31	0.016	1	1	0	0
30	**11**	0.030	0.98	0.047	0.259	0.33	0.016	1	1	0	0
31	**11**	0.029	0.98	0.033	0.246	0.31	0.016	1	1	0	0
32	**11**	0.035	0.98	0.033	0.246	0.31	0.022	1	1	0	0
33	**11**	0.038	0.98	0.034	0.239	0.31	0.022	1	1	0	0
34	**11**	0.034	0.98	0.047	0.259	0.33	0.022	1	1	0	0
35	**11**	0.042	0.25	0.068	0.179	0.25	0.022	1	1	0	0
36	**11**	0.039	0.98	0.034	0.239	0.31	0.028	1	1	0	0

	Reference	d_{se} (m)	d_{50} (mm)	y (m)	U (m/s)	U_c (m/s)	D (m)	m	n	S_m (m)	S_n (m)
37	**11**	0.051	0.98	0.048	0.254	0.33	0.028	1	1	0	0
38	**11**	0.046	0.25	0.068	0.179	0.25	0.028	1	1	0	0
39	**11**	0.054	0.25	0.068	0.179	0.25	0.031	1	1	0	0
40	**11**	0.047	0.98	0.034	0.239	0.31	0.016	4	2	0.016	0.016
41	**11**	0.045	0.98	0.035	0.232	0.31	0.016	4	2	0.018	0.0184
42	**11**	0.049	0.98	0.034	0.239	0.31	0.016	4	2	0.020	0.02
43	**11**	0.045	0.98	0.034	0.239	0.31	0.016	4	2	0.024	0.024
44	**11**	0.032	0.98	0.034	0.239	0.31	0.016	4	2	0.048	0.048
45	**11**	0.031	0.98	0.035	0.232	0.31	0.016	4	2	0.048	0.048
46	**11**	0.028	0.98	0.035	0.232	0.31	0.016	4	2	0.080	0.08
47	**11**	0.028	0.98	0.035	0.232	0.31	0.016	4	2	0.080	0.08
48	**11**	0.055	0.98	0.045	0.271	0.32	0.016	4	2	0.016	0.016
49	**11**	0.056	0.98	0.047	0.259	0.33	0.016	4	2	0.018	0.0184
50	**11**	0.053	0.98	0.047	0.259	0.33	0.016	4	2	0.020	0.02
51	**11**	0.050	0.98	0.046	0.265	0.33	0.016	4	2	0.024	0.024
52	**11**	0.037	0.98	0.047	0.259	0.33	0.016	4	2	0.048	0.048
53	**11**	0.032	0.98	0.048	0.254	0.33	0.016	4	2	0.080	0.08
54	**11**	0.031	0.98	0.047	0.259	0.33	0.016	4	2	0.096	0.096
55	**11**	0.040	0.98	0.048	0.254	0.33	0.016	4	2	0.048	0.048
56	**11**	0.037	0.98	0.054	0.225	0.34	0.016	4	2	0.080	0.08
57	**11**	0.039	0.98	0.055	0.221	0.34	0.016	4	2	0.048	0.048
58	**11**	0.055	0.98	0.034	0.239	0.31	0.022	4	2	0.022	0.022
59	**11**	0.048	0.98	0.035	0.232	0.31	0.022	4	2	0.025	0.0253
60	**11**	0.064	0.98	0.038	0.213	0.33	0.022	4	2	0.028	0.0275
61	**11**	0.053	0.98	0.034	0.239	0.31	0.022	4	2	0.033	0.033
62	**11**	0.044	0.98	0.034	0.239	0.31	0.022	4	2	0.066	0.066
63	**11**	0.042	0.98	0.035	0.232	0.31	0.022	4	2	0.066	0.066
64	**11**	0.033	0.98	0.034	0.239	0.31	0.022	4	2	0.110	0.11
65	**11**	0.065	0.98	0.044	0.277	0.33	0.022	4	2	0.022	0.022
66	**11**	0.057	0.98	0.046	0.265	0.33	0.022	4	2	0.025	0.0253
67	**11**	0.064	0.98	0.047	0.259	0.33	0.022	4	2	0.028	0.0275
68	**11**	0.059	0.98	0.048	0.254	0.33	0.022	4	2	0.033	0.033
69	**11**	0.048	0.98	0.048	0.254	0.33	0.022	4	2	0.066	0.066
70	**11**	0.038	0.98	0.048	0.254	0.33	0.022	4	2	0.110	0.11
71	**11**	0.025	0.98	0.035	0.232	0.31	0.022	4	2	0.110	0.11
72	**11**	0.052	0.98	0.054	0.225	0.34	0.022	4	2	0.066	0.066

	Reference	d_{se} (m)	d_{50} (mm)	y (m)	U (m/s)	U_c (m/s)	D (m)	m	n	S_m (m)	S_n (m)
73	**11**	0.042	0.98	0.055	0.221	0.34	0.022	4	2	0.110	0.11
74	**11**	0.067	0.98	0.047	0.259	0.33	0.028	4	2	0.035	0.035
75	**11**	0.048	0.98	0.035	0.232	0.31	0.016	3	2	0.020	0.02
76	**11**	0.045	0.98	0.035	0.232	0.31	0.016	3	2	0.020	0.02
77	**11**	0.043	0.98	0.033	0.246	0.31	0.016	3	2	0.024	0.024
78	**11**	0.035	0.98	0.033	0.246	0.31	0.016	3	2	0.048	0.048
79	**11**	0.050	0.98	0.047	0.259	0.33	0.016	3	2	0.020	0.02
80	**11**	0.036	0.98	0.038	0.267	0.31	0.016	3	2	0.048	0.048
81	**11**	0.030	0.98	0.033	0.246	0.31	0.016	3	2	0.080	0.08
82	**11**	0.036	0.98	0.040	0.254	0.32	0.016	3	2	0.048	0.048
83	**11**	0.050	0.98	0.034	0.239	0.31	0.022	3	2	0.028	0.0275
84	**11**	0.038	0.98	0.034	0.239	0.31	0.022	3	2	0.028	0.0275
85	**11**	0.059	0.98	0.039	0.264	0.32	0.022	3	2	0.028	0.0275
86	**11**	0.040	0.98	0.050	0.243	0.33	0.022	3	2	0.028	0.0275
87	**11**	0.057	0.25	0.068	0.179	0.25	0.022	3	2	0.028	0.0275
88	**11**	0.054	0.25	0.068	0.179	0.25	0.022	3	2	0.044	0.044
89	**11**	0.051	0.25	0.068	0.179	0.25	0.022	3	2	0.066	0.066
90	**11**	0.048	0.98	0.068	0.179	0.25	0.022	3	2	0.110	0.11
91	**11**	0.047	0.98	0.034	0.239	0.31	0.016	2	2	0.020	0.02
92	**11**	0.034	0.98	0.033	0.246	0.31	0.016	2	2	0.048	0.048
93	**11**	0.043	0.98	0.033	0.246	0.31	0.016	2	2	0.024	0.024
94	**11**	0.046	0.98	0.033	0.254	0.31	0.016	2	2	0.024	0.024
95	**11**	0.032	0.98	0.033	0.246	0.31	0.016	2	2	0.080	0.08
96	**11**	0.029	0.98	0.033	0.246	0.31	0.016	2	2	0.096	0.096
97	**11**	0.034	0.98	0.035	0.232	0.31	0.016	2	2	0.020	0.02
98	**11**	0.038	0.98	0.043	0.283	0.32	0.016	2	2	0.048	0.048
99	**11**	0.023	0.98	0.044	0.277	0.33	0.016	2	2	0.096	0.096
100	**11**	0.044	0.98	0.048	0.254	0.33	0.016	2	2	0.024	0.024
101	**11**	0.049	0.98	0.049	0.248	0.33	0.016	2	2	0.020	0.02
102	**11**	0.040	0.98	0.034	0.239	0.31	0.022	2	2	0.028	0.0275
103	**11**	0.057	0.98	0.038	0.213	0.31	0.022	2	2	0.028	0.0275
104	**11**	0.066	0.98	0.040	0.257	0.32	0.022	2	2	0.028	0.0275
105	**11**	0.062	0.98	0.050	0.243	0.33	0.022	2	2	0.028	0.0275
106	**11**	0.056	0.25	0.068	0.179	0.25	0.022	2	2	0.028	0.0275
107	**11**	0.049	0.25	0.068	0.179	0.25	0.022	2	2	0.044	0.044
108	**11**	0.048	0.25	0.068	0.179	0.25	0.022	2	2	0.066	0.066

	Reference	d_{se} (m)	d_{50} (mm)	y (m)	U (m/s)	U_c (m/s)	D (m)	m	n	S_m (m)	S_n (m)
109	**11**	0.046	0.25	0.068	0.179	0.25	0.022	2	2	0.110	0.11
110	**11**	0.058	0.98	0.033	0.246	0.31	0.016	2	3	0.020	0.02
111	**11**	0.052	0.98	0.033	0.246	0.31	0.016	2	3	0.024	0.024
112	**11**	0.034	0.98	0.033	0.246	0.31	0.016	2	3	0.048	0.048
113	**11**	0.031	0.98	0.033	0.246	0.31	0.016	2	3	0.080	0.08
114	**11**	0.055	0.25	0.068	0.179	0.25	0.022	2	3	0.044	0.044
115	**11**	0.053	0.25	0.068	0.179	0.25	0.022	2	3	0.066	0.066
116	**11**	0.040	0.98	0.047	0.259	0.33	0.016	1	2	0	0.024
117	**11**	0.037	0.98	0.047	0.259	0.33	0.016	1	2	0	0.032
118	**11**	0.035	0.98	0.047	0.259	0.33	0.016	1	2	0	0.048
119	**11**	0.032	0.98	0.047	0.259	0.33	0.016	1	2	0	0.08
120	**11**	0.031	0.98	0.047	0.259	0.33	0.016	1	2	0	0.112
121	**11**	0.062	0.25	0.068	0.179	0.25	0.022	1	2	0	0.028
122	**11**	0.051	0.25	0.068	0.179	0.25	0.022	1	2	0	0.044
123	**11**	0.048	0.25	0.068	0.179	0.25	0.022	1	2	0	0.066
124	**11**	0.045	0.25	0.068	0.179	0.25	0.022	1	2	0	0.11
125	**11**	0.032	0.98	0.047	0.259	0.33	0.016	2	1	0.024	0
126	**11**	0.031	0.98	0.047	0.259	0.33	0.016	2	1	0.048	0
127	**11**	0.032	0.98	0.047	0.259	0.33	0.016	2	1	0.080	0
128	**11**	0.032	0.98	0.047	0.259	0.33	0.016	2	1	0.112	0
129	**11**	0.030	0.98	0.047	0.259	0.33	0.016	2	1	0.032	0
130	**11**	0.030	0.98	0.047	0.259	0.33	0.016	2	1	0.048	0
131	**11**	0.041	0.98	0.034	0.239	0.31	0.022	2	1	0.066	0
132	**11**	0.040	0.98	0.034	0.239	0.31	0.022	2	1	0.110	0
133	**11**	0.042	0.98	0.034	0.239	0.31	0.022	2	1	0.044	0
134	**11**	0.041	0.25	0.068	0.179	0.25	0.022	2	1	0.028	0
135	**11**	0.047	0.25	0.068	0.179	0.25	0.022	2	1	0.044	0
136	**11**	0.048	0.25	0.068	0.179	0.25	0.022	2	1	0.066	0
137	**11**	0.045	0.25	0.068	0.179	0.25	0.022	2	1	0.110	0
138	**11**	0.048	0.25	0.068	0.179	0.25	0.022	3	1	0.066	0
139	**11**	0.048	0.25	0.068	0.179	0.25	0.022	4	1	0.066	0
140	**12**	0.153	0.86	0.200	0.310	0.32	0.05	4	1	0.050	0
141	**12**	0.160	0.86	0.200	0.310	0.32	0.05	4	1	0.100	0
142	**12**	0.152	0.86	0.200	0.310	0.32	0.05	4	1	0.150	0
143	**12**	0.149	0.86	0.200	0.310	0.32	0.05	4	1	0.225	0
144	**12**	0.136	0.86	0.200	0.310	0.32	0.05	4	1	0.300	0

	Reference	d_{se} (m)	d_{50} (mm)	y (m)	U (m/s)	U_c (m/s)	D (m)	m	n	S_m (m)	S_n (m)
145	**12**	0.261	0.86	0.200	0.310	0.32	0.05	4	2	0.050	0.05
146	**12**	0.185	0.86	0.200	0.310	0.32	0.05	4	2	0.100	0.1
147	**12**	0.183	0.86	0.200	0.310	0.32	0.05	4	2	0.150	0.15
148	**12**	0.146	0.86	0.200	0.310	0.32	0.05	4	2	0.225	0.225
149	**12**	0.156	0.86	0.200	0.310	0.32	0.05	4	2	0.300	0.3
150	**12**	0.327	0.86	0.200	0.310	0.32	0.05	4	3	0.050	0.05
151	**12**	0.211	0.86	0.200	0.310	0.32	0.05	4	3	0.100	0.1
152	**12**	0.208	0.86	0.200	0.310	0.32	0.05	4	3	0.150	0.15
153	**12**	0.218	0.86	0.200	0.310	0.32	0.05	4	3	0.225	0.225
154	**12**	0.139	0.86	0.200	0.310	0.32	0.05	4	3	0.300	0.3
155	**12**	0.354	0.86	0.200	0.310	0.32	0.05	1	4	0	0.05
156	**12**	0.190	0.86	0.200	0.310	0.32	0.05	1	4	0	0.1
157	**12**	0.175	0.86	0.200	0.310	0.32	0.05	1	4	0	0.15
158	**12**	0.159	0.86	0.200	0.310	0.32	0.05	1	4	0	0.225
159	**12**	0.127	0.86	0.200	0.310	0.32	0.05	1	4	0	0.3
160	**12**	0.369	0.86	0.200	0.310	0.32	0.05	2	4	0.050	0.05
161	**12**	0.212	0.86	0.200	0.310	0.32	0.05	2	4	0.100	0.1
162	**12**	0.189	0.86	0.200	0.310	0.32	0.05	2	4	0.150	0.15
163	**12**	0.178	0.86	0.200	0.310	0.32	0.05	2	4	0.225	0.225
164	**12**	0.141	0.86	0.200	0.310	0.32	0.05	2	4	0.300	0.3
165	**12**	0.328	0.86	0.200	0.310	0.32	0.05	3	4	0.050	0.05
166	**12**	0.255	0.86	0.200	0.310	0.32	0.05	3	4	0.100	0.1
167	**12**	0.187	0.86	0.200	0.310	0.32	0.05	3	4	0.150	0.15
168	**12**	0.151	0.86	0.200	0.310	0.32	0.05	3	4	0.225	0.225
169	**12**	0.145	0.86	0.200	0.310	0.32	0.05	3	4	0.300	0.3
170	**13**	0.183	0.8	0.240	0.365	0.38	0.06	2	2	0.060	0.06
171	**13**	0.148	0.8	0.240	0.369	0.38	0.06	2	2	0.090	0.09
172	**13**	0.129	0.8	0.240	0.369	0.38	0.06	2	2	0.120	0.12
173	**13**	0.108	0.8	0.240	0.365	0.38	0.06	2	2	0.150	0.15
174	**13**	0.104	0.8	0.240	0.365	0.38	0.06	2	2	0.180	0.18
175	**13**	0.098	0.8	0.240	0.365	0.38	0.06	2	2	0.240	0.24
176	**13**	0.098	0.8	0.240	0.361	0.38	0.06	2	2	0.290	0.29
177	**13**	0.099	0.8	0.240	0.365	0.38	0.06	2	2	0.330	0.33
178	**13**	0.238	0.8	0.240	0.361	0.38	0.06	5	3	0.060	0.06
179	**13**	0.180	0.8	0.240	0.361	0.38	0.06	5	3	0.075	0.075
180	**13**	0.171	0.8	0.240	0.361	0.38	0.06	5	3	0.090	0.09

	Reference	d_{se} (m)	d_{50} (mm)	y (m)	U (m/s)	U_c (m/s)	D (m)	m	n	S_m (m)	S_n (m)
181	**13**	0.150	0.8	0.240	0.361	0.38	0.06	5	3	0.120	0.12
182	**13**	0.130	0.8	0.240	0.365	0.38	0.06	5	3	0.150	0.15
183	**13**	0.115	0.8	0.240	0.361	0.38	0.06	5	3	0.180	0.18
184	**13**	0.110	0.8	0.240	0.365	0.38	0.06	5	3	0.210	0.21
185	**13**	0.107	0.8	0.240	0.361	0.38	0.06	5	3	0.250	0.25
186	**13**	0.105	0.8	0.240	0.365	0.38	0.06	5	3	0.300	0.3
187	**13**	0.104	0.8	0.240	0.361	0.38	0.06	5	3	0.330	0.33
188	**13**	0.150	0.8	0.240	0.361	0.38	0.042	4	2	0.042	0.042
189	**13**	0.128	0.8	0.240	0.361	0.38	0.042	4	2	0.060	0.06
190	**13**	0.108	0.8	0.240	0.361	0.38	0.042	4	2	0.084	0.084
191	**13**	0.090	0.8	0.240	0.361	0.38	0.042	4	2	0.120	0.12
192	**13**	0.085	0.8	0.240	0.361	0.38	0.042	4	2	0.150	0.15
193	**13**	0.081	0.8	0.240	0.361	0.38	0.042	4	2	0.189	0.189
194	**13**	0.077	0.8	0.240	0.361	0.38	0.042	4	2	0.230	0.23
195	**13**	0.254	0.8	0.240	0.365	0.38	0.06	4	3	0.060	0.06
196	**13**	0.223	0.8	0.240	0.365	0.38	0.06	4	3	0.080	0.08
197	**13**	0.183	0.8	0.240	0.365	0.38	0.06	4	3	0.100	0.1
198	**13**	0.169	0.8	0.240	0.365	0.38	0.06	4	3	0.120	0.12
199	**13**	0.147	0.8	0.240	0.361	0.38	0.06	4	3	0.150	0.15
200	**13**	0.134	0.8	0.240	0.365	0.38	0.06	4	3	0.180	0.18
201	**13**	0.130	0.8	0.240	0.361	0.38	0.06	4	3	0.210	0.21
202	**13**	0.120	0.8	0.240	0.361	0.38	0.06	4	3	0.250	0.25
203	**13**	0.119	0.8	0.240	0.361	0.38	0.06	4	3	0.300	0.3
204	**13**	0.200	0.8	0.240	0.365	0.38	0.042	5	3	0.042	0.042
205	**13**	0.154	0.8	0.240	0.365	0.38	0.042	5	3	0.062	0.062
206	**13**	0.123	0.8	0.240	0.365	0.38	0.042	5	3	0.102	0.102
207	**13**	0.103	0.8	0.240	0.361	0.38	0.042	5	3	0.150	0.15
208	**13**	0.098	0.8	0.240	0.361	0.38	0.042	5	3	0.200	0.2
209	**13**	0.097	0.8	0.240	0.361	0.38	0.042	5	3	0.240	0.24
210	**13**	0.199	0.8	0.240	0.365	0.38	0.06	2	2	0.060	0.06
211	**13**	0.121	0.8	0.240	0.365	0.38	0.06	2	2	0.060	0.12
212	**13**	0.134	0.8	0.240	0.365	0.38	0.06	2	2	0.090	0.12
213	**13**	0.117	0.8	0.240	0.365	0.38	0.06	2	2	0.140	0.12
214	**13**	0.125	0.8	0.240	0.361	0.38	0.06	2	2	0.180	0.12
215	**13**	0.139	0.8	0.240	0.365	0.38	0.06	2	2	0.210	0.12
216	**13**	0.129	0.8	0.240	0.365	0.38	0.06	2	2	0.240	0.12

	Reference	d_{se} (m)	d_{50} (mm)	y (m)	U (m/s)	U_c (m/s)	D (m)	m	n	S_m (m)	S_n (m)
217	**13**	0.123	0.8	0.240	0.376	0.38	0.06	2	2	0.270	0.12
218	**13**	0.210	0.8	0.240	0.365	0.38	0.06	5	3	0.060	0.06
219	**13**	0.148	0.8	0.240	0.365	0.38	0.06	5	3	0.060	0.12
220	**13**	0.163	0.8	0.240	0.361	0.38	0.06	5	3	0.090	0.12
221	**13**	0.165	0.8	0.240	0.361	0.38	0.06	5	3	0.110	0.12
222	**13**	0.168	0.8	0.240	0.361	0.38	0.06	5	3	0.140	0.12
223	**13**	0.172	0.8	0.240	0.361	0.38	0.06	5	3	0.180	0.12
224	**13**	0.176	0.8	0.240	0.365	0.38	0.06	5	3	0.210	0.12
225	**13**	0.153	0.8	0.240	0.365	0.38	0.06	5	3	0.240	0.12
226	**13**	0.150	0.8	0.240	0.361	0.38	0.06	5	3	0.270	0.12
227	**13**	0.200	0.8	0.240	0.365	0.38	0.06	2	2	0.120	0.06
228	**13**	0.148	0.8	0.240	0.361	0.38	0.06	2	2	0.120	0.09
229	**13**	0.132	0.8	0.240	0.365	0.38	0.06	2	2	0.120	0.12
230	**13**	0.120	0.8	0.240	0.361	0.38	0.06	2	2	0.120	0.16
231	**13**	0.110	0.8	0.240	0.361	0.38	0.06	2	2	0.120	0.19
232	**13**	0.106	0.8	0.240	0.361	0.38	0.06	2	2	0.120	0.21
233	**13**	0.110	0.8	0.240	0.365	0.38	0.06	2	2	0.120	0.24
234	**13**	0.107	0.8	0.240	0.361	0.38	0.06	2	2	0.120	0.27
235	**13**	0.270	0.8	0.240	0.365	0.38	0.06	5	3	0.120	0.06
236	**13**	0.200	0.8	0.240	0.361	0.38	0.06	5	3	0.120	0.09
237	**13**	0.172	0.8	0.240	0.365	0.38	0.06	5	3	0.120	0.12
238	**13**	0.160	0.8	0.240	0.372	0.38	0.06	5	3	0.120	0.15
239	**13**	0.137	0.8	0.240	0.361	0.38	0.06	5	3	0.120	0.21
240	**13**	0.144	0.8	0.240	0.365	0.38	0.06	5	3	0.120	0.21
241	**13**	0.137	0.8	0.240	0.369	0.38	0.06	5	3	0.120	0.27
242	**14**	0.062	0.75	0.140	0.285	0.40	0.033	2	1	0.033	0
243	**14**	0.064	0.75	0.140	0.285	0.40	0.033	2	1	0.052	0
244	**14**	0.070	0.75	0.140	0.285	0.40	0.033	2	1	0.068	0
245	**14**	0.072	0.75	0.140	0.285	0.40	0.033	2	1	0.101	0
246	**14**	0.068	0.75	0.140	0.285	0.40	0.033	2	1	0.135	0
247	**14**	0.068	0.75	0.140	0.285	0.40	0.033	2	1	0.160	0
248	**14**	0.067	0.75	0.140	0.285	0.40	0.033	2	1	0.200	0
249	**14**	0.065	0.75	0.140	0.285	0.40	0.033	2	1	0.266	0
250	**14**	0.064	0.75	0.140	0.285	0.40	0.033	2	1	0.364	0
251	**14**	0.062	0.75	0.140	0.285	0.40	0.033	2	1	0.530	0
252	**14**	0.062	0.75	0.140	0.285	0.40	0.033	2	1	0.695	0

	Reference	d_{se} (m)	d_{50} (mm)	y (m)	U (m/s)	U_c (m/s)	D (m)	m	n	S_m (m)	S_n (m)
253	**14**	0.120	0.75	0.140	0.285	0.40	0.033	1	2	0	0.035
254	**14**	0.073	0.75	0.140	0.285	0.40	0.033	1	2	0	0.069
255	**14**	0.066	0.75	0.140	0.285	0.40	0.033	1	2	0	0.136
256	**14**	0.068	0.75	0.140	0.285	0.40	0.033	1	2	0	0.164
257	**14**	0.068	0.75	0.140	0.285	0.40	0.033	1	2	0	0.202
258	**14**	0.064	0.75	0.140	0.285	0.40	0.033	1	2	0	0.229
259	**14**	0.064	0.75	0.140	0.285	0.40	0.033	1	2	0	0.267
260	**14**	0.064	0.75	0.140	0.285	0.40	0.033	1	2	0	0.363
261	**15**	0.068	0.17	0.213	0.180	0.28	0.0318	3	8	0.095	0.0954
262	**15**	0.081	0.17	0.215	0.180	0.28	0.0318	8	3	0.095	0.0954
263	**15**	0.095	0.17	0.211	0.170	0.27	0.0318	3	8	0.095	0.0954
264	**16**	0.132	0.172	0.381	0.240	0.28	0.0318	8	3	0.095	0.0953
265	**16**	0.241	0.22	1.201	0.330	0.32	0.0318	3	8	0.095	0.0953
266	**16**	0.085	0.172	0.381	0.230	0.28	0.0318	4	2	0.095	0.0953
267	**16**	0.089	0.172	0.381	0.230	0.26	0.0318	1	3	0.095	0.0953
268	**16**	0.122	0.172	0.381	0.280	0.27	0.0318	3	3	0.095	0.0953
269	**16**	0.114	0.172	0.378	0.230	0.27	0.0318	5	3	0.095	0.0953

Table 3. Range of different variables used in this study.

Variables	Range
Flow depth (y)	0.033-1.201 (m)
Flow mean velocity (U)	0.170-0.433 (m/s)
Critical velocity (U_c)	0.250-0.530 (m/s)
Grains mean diameter (d_{50})	0.17-2.4 (mm)
Pile diameter (D)	0.016-0.06 (m)
Center to center spacing of the piles inline to flow (S_m)	0-0.695 (m)
Center to center spacing of the piles inline to flow (S_n)	0-0.363 (m)
Number of piles inline with flow (m)	1-8
Number of piles normal to the flow (n)	1-8
Equilibrium scour depth (d_{se})	0.0213-0.369 (m)

The whole dataset of 269 points was divided into training and testing datasets. 80% of the data was used to train the model, and the remaining 20% were utilized to test it. Initially, the training data set was fed into both the MARS and GEP models to generate an equation between the input variables and the output variable (i.e. scour depth). Once this equation is generated, it is used to predict the scour depth from the testing input variables. Performance of the MARS and GEP models is assessed via three statistical metrics, namely mean absolute error (MAE), root mean square error (RMSE), and correlation coefficient (R^2). These metrics are given by,

$$\text{MAE} = \frac{1}{N}\sum_{i=1}^{N}|O_i - P_i| \tag{4}$$

$$\text{RMSE} = \sqrt{\frac{\sum_{i=1}^{N}(O_i - P_i)^2}{N}} \tag{5}$$

$$\text{R}^2 = \frac{\sum_{i=1}^{N}(O_i - \bar{O})(P_i - \bar{P})}{\sqrt{\sum_{i=1}^{N}(O_i - \bar{O})^2 \sum_{i=1}^{N}(P_i - \bar{P})^2}} \tag{6}$$

where N is the number of observations, O_i and P_i are respectively the observed and predicted values, and the bar denotes the average of the variable.

3. Previous Studies: Commonly Used Empirical Relations

Richardson and Davis (2001) proposed the following empirical formula for the estimation of scour depth around single piles:

$$\frac{S}{D^*} = 2.0K_1K_2K_3K_4\left(\frac{h}{D}\right)^{0.35} Fr^{0.43} \quad (7)$$

where K_1 is the correction factor for pier nose shape (**Figure 6** and **Table 4**), K_2 is the correction factor for angle of attack (**Table 5**), $K_3$is the coefficient factor based on the channel bed condition (**Table 6**), and K_4 is the correction factor for armoring by bed material size, and Fr is the Froude number. Streamlining the upstream end of a pier reduces the strength of the horseshoe vortex. Streamlining the downstream end of piers reduces the strength of the wake vortices. A square-nose pier has a scour depth 20% greater than a sharp-nose pier and 10% larger than a cylindrical or round-nose pier.

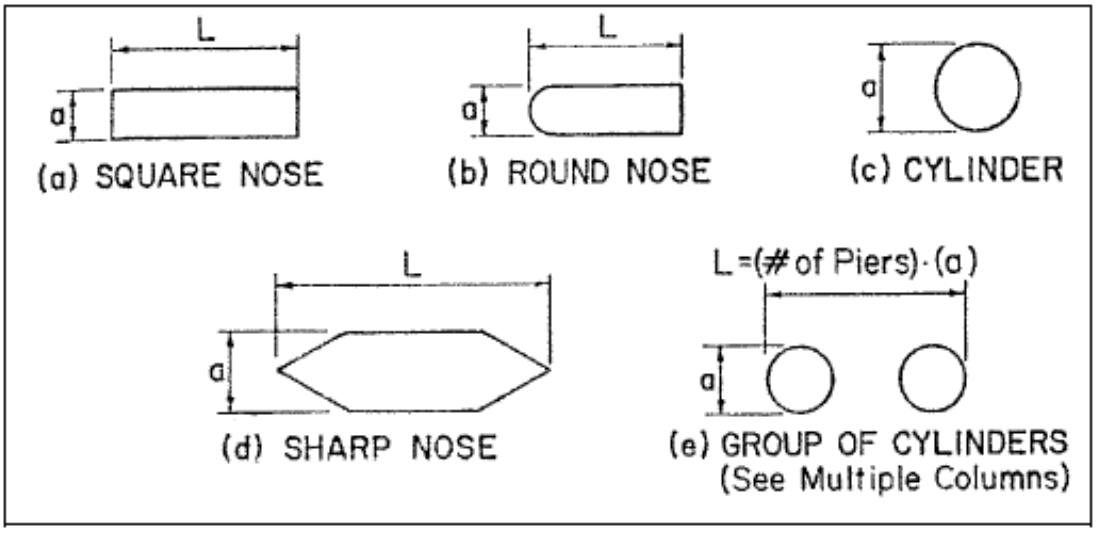

Figure 6. Different pier nose shapes (Richardson and Davis, 2001).

In this study, L, or groups of cylinders, was used for the shape of the pier nose (K_1 = 1). The angle of attack (θ) was set to 0^o because the flow in the flume was in line with the piers. K_3 was set to 1.1 for a laboratory set condition of clear – water scour.

Table 4. K_1 correction factor for different pier nose shapes (Richardson and Davis, 2001).

Index	Shape of pier nose	K_1
(a)	Square nose	1.1
(b)	Round nose	1.0
(c)	Circular nose	1.0
(d)	Group of cylinders	1.0
(e)	Sharp nose	0.9

Another relevant variable in the prediction of scour depth (not examined in this study) is the angle of attack of the flow to the pier. Angle of attack or the angle at which the flow approaches the pile is reduced when piles are at angles downstream and increased when embankments are at angles upstream. According to Ahmad (1953), the scour depth at a pile inclined 45^o downstream, to the flow of water is reduced by 20%. While, the scour at a pile inclined 45^o upstream, of the flow of water is increased by nearly 10%. Shape of the nose of the pile changes the scour depth by 20% (Richardson and Davis, 2001).

Table 5. K_2 correction factor for angle of attack (Richardson and Davis, 2001).

	K_2		
Angle	L/a = 4	L/a = 8	L/a = 12
0	1.00	1.00	1.00
15	1.50	2.00	2.50
30	2.00	2.75	3.50
45	2.30	3.30	4.30
90	2.50	3.90	5.00

Table 6. K_3 coefficient factor based on the channel bed condition (Richardson and Davis, 2001)

Bed condition	Dune Height (m)	K_3
Clear - water scour	N/A	1.1
Plane bed and antidune flow	N/A	1.1
Small dunes	$0.6 \leq H < 3$	1.1
Medium dunes	$3 < H \leq 9$	1.2 to 1.1
Large dunes	$H \geq 9$	1.3

The correction factor K_4 decreases the scour depth due to armoring of the scour hole for bed materials that have a d_{50} equal to or larger than 2.0 mm and d_{95} equal to or larger than 20 mm. Richardson and Davis (2001) showed that when the flow velocity is less that the critical flow velocity for d_{90} and there is a gradation in sizes in the bed material, the d_{90} will limit the scour depth. In our study, d_{50} was less than 2.0 mm, and therefore $K_4 = 1$.

Ataie-Ashtiani and Beheshti (2006) added a correction factor (K_{Gmn}) to the Richardson and Davis (2001) and developed the following expression for the estimation of scour depth,

$$\frac{d_{se}}{D^*} = 2.0K_1K_2K_3K_4\left(\frac{h}{D}\right)^{0.35} Fr^{0.43}\ K_{Gmn} \tag{8}$$

$$K_{Gmn} = 1.11\left(\frac{m^{0.0396}}{n^{0.5225\times(G/D)^{0.1153}}}\right) \tag{9}$$

where G is the effective pile spacing. The effective width of the pile group (D^*) is calculated by:

$$D^* = D_{proj}K_GK_m \tag{10}$$

where D_{proj} is the sum of the non-overlapping projected widths of the piles, K_G is the coefficient for pile spacing and K_m is the coefficient for the number of aligned rows (Richardson and Davis, 2001).

Ataie-Ashtiani and Beheshti (2006) showed that their equation can estimate the scour depth more accurately than that of the Richardson and Davis (2001). In a similar effort, Howard and Etemad-Shahidi (2014) proposed the following expression for predicting scour depth,

$$\frac{d_{se}}{D} = 2.74(D^2/(S_m^2 + S_n^2))^{0.21}(y/D)^{0.26}Fr^{0.37}n^{0.07} \quad (11)$$

The Colorado State University (CSU) introduced a simple equation for estimation of scour depth, which is given by,

$$d_{se} = 2.0k_1k_2a^{0.65}y^{0.35}Fr^{0.43} \quad (12)$$

where *a* is the pier width. In this equation, the scour depth depends on the Froude number, pier width, pier shape and angle of attack. This equation was the foundation of the research conducted by (Richardson and Davis, 2001).

4. Methodology

4.1. Gene Expression Programming (GEP)

Gene Expression Programming (GEP) is an extension of genetic programming (GP) and the genetic algorithm (GA). GA is a class of problem-solving techniques based on Darwinian theory of evolution by "natural selection". The GA uses common biological principals of genetics. In the GA, the genes are connected together in long strings, called chromosomes. These chromosomes can either be subsets of a function, or the function itself. Each gene, or variable, represents a specific trait of the organism, or predicted function.

An example of the GA is determined by the following objective function:

$$F = \sum_{i=1}^{N} \left(d_{se,measured} - d_{se,estimated} \right)^2 \quad (13)$$

where $d_{se,measured}$ and $d_{se,estimated}$ are respectively the measured and estimated scour depth. The goal of the GA is to minimize the function *F*. For the given example, $S_{estimated}$ is determined by the equation:

$$d_{se,estimated} = aD^{\beta} + bU^{\alpha} + cU_c{}^{\gamma} + dy^{\delta} + em^{\mu} \quad (14)$$

where *D*, *U*, U_c, *y* and *m*, as discussed, could represent the variables affecting scour depth, and *a*, *b, c, d, e,* β, α, γ, δ and μ are the empirical coefficients.

For this example, the GA creates many initial guesses or genes (by a random number generation) for the empirical coefficients. This set of numbers is defined as the GA's first population, which includes the first pool of genes. These genes will then be converted to binary strings of numbers to form the initial population of chromosomes. As an example, the GA will perform the following steps:

1) Test each chromosome to see its performance and assessing its fitness score. The fitness score is a measure of how good the chromosome can estimate $d_{se,estimated}$.
2) Convert each chromosome to a binary code, which is a collection of bits. A bit has a single binary value, either 0 or 1.
3) Select two chromosomes from the current population. The chance of being selected is proportional to the chromosome's fitness.
4) Depending on the crossover rate (the chance that two chromosomes swap their bits), crossover may occur. If the crossover rate is sufficient, the crossover of the bits from the chosen chromosomes will occur at a randomly selected point.
5) This process will step through each of the chosen chromosomes bits, step by step or bit by bit, and flip the bits, depending on the mutation rate (the chance that a bit within a chromosome will be flipped, i.e., 0 becomes 1, and 1 becomes 0). The mutation rate typically ranges from 0.005 to 0.05 (Satar and Gharabaghi, 2015).
6) Repeat steps 1-5 until a new population of chromosomes has been created that best minimizes the function *F*.

As explained above, GA searches within a population of solutions (chromosomes) for the "fittest" solution. In each iteration, GA eliminates poor solutions via the above steps. This improves the quality of chromosomes in the gene pool.

Gene-Expression Programming (GEP) was invented by Ferreira in1999 (Ferrerira, 2001). To express the genetic information encoded in the gene, Ferreira (2001) used expression tree (ET) representations. The gene consists of a head and a tail. The tail of the gene is a sequence of terminals that are extremely important because they allow the modification of the next generations of genes using any genetic operator without restrictions. GEP randomly selects the sequence. For

each problem, the length of the head (h) is chosen, whereas the length of the tail (t_g) is a function of the length of the head (h) and the number of data points (N):

$$t_g = h(N-1)+1 \tag{15}$$

For each problem, the optimum parameter setting for the GEP model is determined by trial and error. Typical values of these parameters are shown in Table 4. Based on these parameters, the GEP creates a random distribution of functions and terminals in the chromosome genes, as GA creates a random set of genes within a population of chromosomes. The first created individual (i.e., chromosome or ET) is random and is called "the parent." The parents are made to yield "offspring" through the implementation of genetic operators such as cross over and mutation. Each individual contributes its own genetic information to the creation of new offspring adapted to the environment with a greater fitness and a higher chance of survival (Satar and Gharabaghi, 2015).

As shown in **Figure 7**, GEP computer programs are encoded in linear chromosomes, which are then expressed or translated into ETs. These computer programs often include mathematical expressions, decision trees, polynomial constructs and logical expressions (Azamathulla, 2012). ETs are sophisticated computer programs that have usually evolved to solve a particular problem, and are selected according to their fitness in solving the problem (Azamathulla, 2012).

Table 7. Typical parameter settings for GEP models (Satar and Gharabaghi, 2015).

Parameter	**Value**
Number of Generations	20,000
Number of Chromosomes	30, 40, 50
Number of Genes	1, 2, 3, 4
Head Size	3, 4, 6
Mutation Rate	0.005 - .05
Crossover Rate	0.1

GEP is a full-fledged genotype/phenotype system with the genotype totally separated from the phenotype. While in GP, genotype and phenotype are mixed together in a simple replicator system. As a result, the fully-fledged genotype/phenotype system of GEP surpasses the old GP system by a factor of 100 – 60,000 (Ferreira 2001a, b).

Reading of ET is done from left to right and down to up. For example, sub-ET 1, sub-ET 2, and sub-ET 3 in Figure 7 are expressed by equations 16, 17 and 18 , respectively:

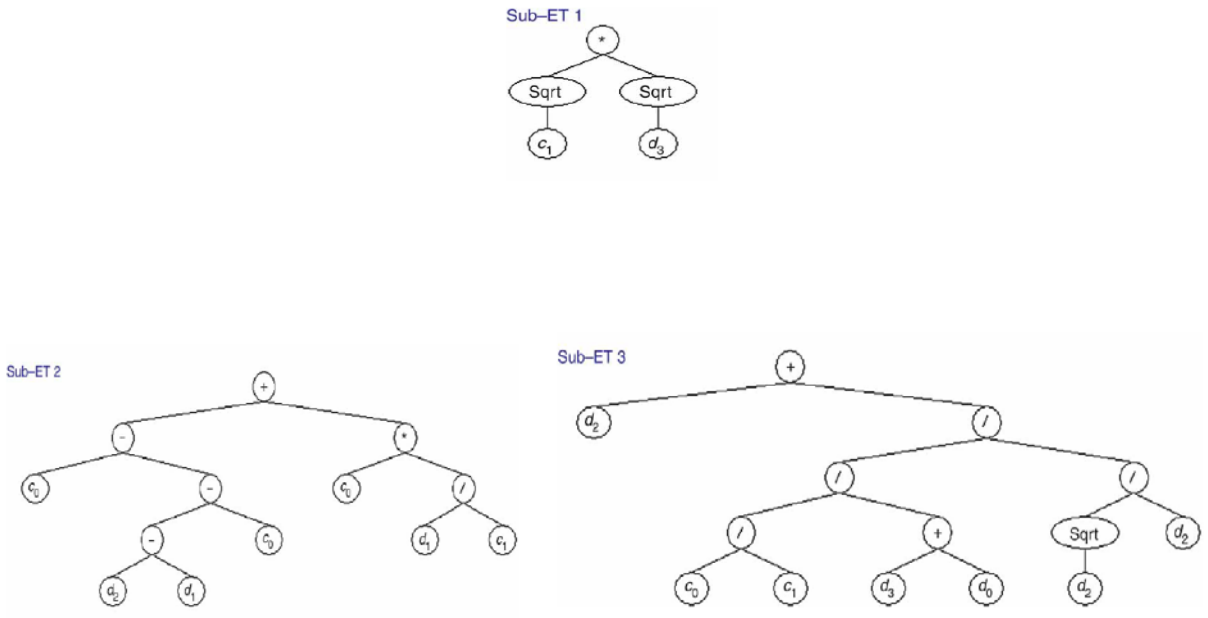

Figure 7. Expression Tree (ET) samples.

$$y = \sqrt{c_1} \times \sqrt{d_3} \tag{16}$$

$$y = \left[c_0 - \left((d_2 - d_1) - c_0\right)\right] + c_0\left(\frac{d_1}{c_1}\right) \tag{17}$$

$$y = d_2 + \left(\frac{{}^{c_0}/_{c_1}}{{}^{\sqrt{d_2}}/_{d_2}}\right) \tag{18}$$

For this study, a GEP-based equation was developed to estimate the scour depth around piles groups. Different steps used for the estimation of scour depth are summarized herein:

1. The first step includes the selection of a fitness function. In this study, the RRSE fitness function of an individual program, *i*, is used (Ferreira, 2001):

$$RRSE_i = \sqrt{\frac{\sum_{j=1}^{N}(P_{ij} - T_j)^2}{\sum_{j=1}^{N}(T_i - \bar{T})^2}} \tag{19}$$

where P_{ij} is the predicted value by the individual chromosome *i* for fitness case *j*, T_i is the target value for fitness case j and $\bar{T}$ is the average of T_j. Thereafter, the fitness of the individual chromosome *i* (T_j) is given by

$$f_i = 1000 \times \frac{1}{1+RRSE_i} \tag{20}$$

where f_i ranges from 0 to 1000 (1000 corresponds to a chromosome with ideal fitness) (Ferreira, 2006).

2. In the second step, a set of terminals (T) and functions (F) must be selected to generate each gene of chromosome. In this study, the terminal set consists of independent variables, namely flow depth and velocity, critical flow velocity, grains mean diameter, and pile diameter. Also, arithmetic and trigonometric functions such as $+, -, \times, /, \sqrt{}$, Sin, Cos, power, ln, and log are used.
3. In the third step, the chromosomal architecture (i.e., the length of the head and the number of genes) is chosen. The head of chromosome contains symbols that represent both terminals (elements from the terminal set) and functions (elements from the function set). The number of genes per chromosome is important because it determines the number of

sub-expression trees (sub-ETs). Ferreira (2001b) showed that the success rate of GEP enhances significantly as the number of gens increases from 1 to 3. Hence, is this study, 3 genes are used per chromosome. Also, different head lengths were used for GEP. The results show that the performance of GEP model does not significantly improve in the training and testing phases when number of genes and head length become larger than 3 and 8, respectively. Thus, the head length (h) and number of genes in each chromosome are set to 8 and 3 in the GEP model. Number of chromosomes is varied from 30 to 50 (Ferreira, 2001b). It is found that the best individuals have 30 chromosomes.

4. In the fourth step, the genetic operators and their rates are selected. This study takes advantage of a combination of genetic operators including mutation and inversion, the three types of transposition (IS, RIS, and gene-transposition), and the three kinds of recombination (one-point, two-point, and gene-recombination).
5. The last step contains choosing a function that links the sub-ETs. Different types of linking functions such as addition (+), subtraction (−), division (/), and multiplication (×) can be used. In this study, the sub-ETs are linked by the addition operators (+) because it gave better results compared to the other operators (i. e., −, /, ×) and has been used widely in other studies (Azamathulla and Jarrett, 2013; Emamgholizadeh et al., 2015).

After selecting the fitness function, and the other required parameters as shown in steps 1 thru 5, the GEP model is run to estimate scour depth. Training of GEP is terminated after 100,000 generations because variations in error are found to be negligible. In other words, after 100,000 generations, the fitness function converges to a value in which no significant changes are observed in it, or the RRSE between two subsequent runs is less than 0.01.: Dimensionless Data Set.

4.2. Multivariate Adaptive Regression Splines (MARS)

MARS is a non-parametric model that was developed by Friedman (1991). MARS looks for patterns within the data and applies linear or cubic functions to simulate those patterns (

Figure 8). As shown in Figure 8, the patterns are captured by three linear functions in different segments. The end points of these segments are called knots. A knot marks the end of one region (segment) of data, and the beginning of another. The resulting piecewise linear or cubic functions (known as basis functions, BFs) between the scour depth and its variables give a greater flexibility to the model.

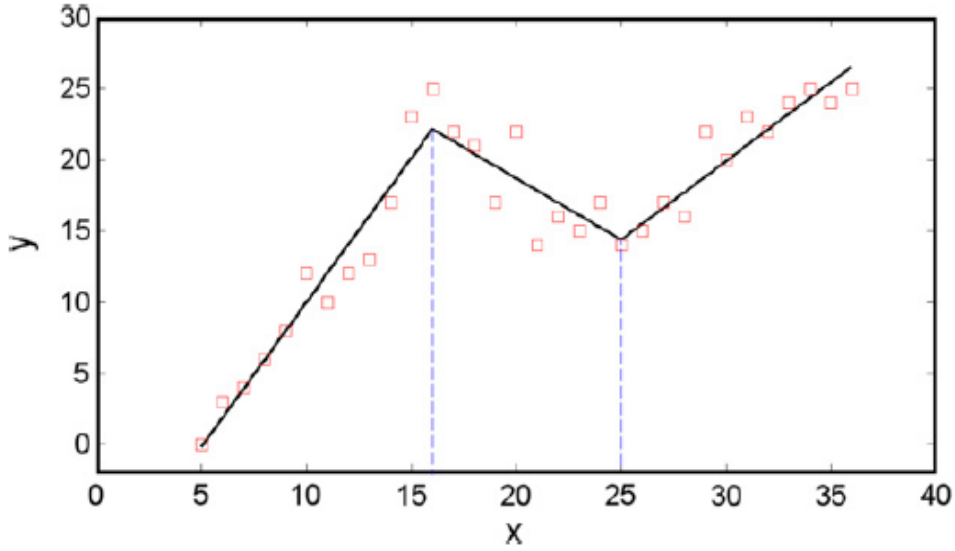

Figure 8. An example of linear splines in MARS.

MARS finds the relationship between the input and output variables through generation of BFs by searching in a stepwise manner. MARS builds the model in two phases: forward selection and backward deletion. Forward selection starts with a model consisting of just the intercept term. Then, MARS iteratively adds reflected pairs of BFs and picks the BF that gives the largest reduction in error. An adaptive regression algorithm is used for selecting the knot locations.

Through the second phase (backward deletion), the large model created in forward selection is trimmed. The aim of the backward deletion procedure is to find a close to optimal model by removing extraneous variables. The backward pass trims the model by removing the basis functions with the lowest contribution to the model until it finds the best sub-model. This process is done through generalized cross validation (GCV) of the basis functions, where the BF with the least importance will be removed from the model. This leaves the model with the lowest GCV and mean squared error (MSE) values. The GCV is a goodness of fit test that penalizes large numbers of BFs and serves to reduce the chance of over fitting (Zhang et al., 2013). It is calculated by,

$$GCV = \frac{MSE_{train}}{\left(1-\frac{enp}{n}\right)^2} \tag{21}$$

where MSE_{train} is the mean square error of the evaluated model, *n* is the number of observations in the training data and *enp* is the effective number of parameters defined by:

$$enp = k + c \times \frac{(k-1)}{2} \tag{22}$$

where k is the number of basis functions in the model that includes the intercept term, and c is a predefined structure of training parameters for the algorithm. $\frac{(k-1)}{2}$ is the number of hinge functions or knots. Therefore the formula not only penalizes the number of basis functions but also the number of knots (Jakabson, 2015). MARS is an adaptive procedure because the selection of BFs and the variable knot locations are data-based and specific to the issue at hand (Zhang et al., 2013).

Once the optimal MARS model is determined, the procedure known as the Analysis of Variance (ANOVA) decompositions can be used to assess the contribution of input variables on the scour depth. This is done by grouping together all BFs that involve that specific variable.

Let *y* be the target output and a matrix of *p* input variables is given by $\boldsymbol{X} = (X_1, \ldots, X_p)$. It is assumed that the output is generated by an unknown "true" model, *f*. For a continuous response, the "true" model is given by:

$$y = f\left(X_1 \ldots, X_p\right) + e = f(\boldsymbol{X}) + e \tag{23}$$

where *e* is the distribution of the error.

The MARS approximation of the function *f* (**X**) is done by applying piecewise linear or cubic BFs. In this study, the focus is on the piecewise linear BF, which is of the form max(0, $x - t$) with a knot occurring at *t*. It can be expressed as:

$$\max(0, x - t) = \begin{cases} x - t, \text{if } x \geq t \\ 0, otherwise \end{cases} \tag{24}$$

The MARS-based function is constructed as a linear combination of BFs and their interactions, and is expressed as:

$$f(X) = \beta_o + \sum_{m=1}^{M} \beta_m B_i(x) \tag{25}$$

The BFs are denoted by $\lambda_m(\boldsymbol{X})$, and *M* is the number of BFs. Each BF is either a single function (called first order BF) or the product of two functions (named second order BF). Higher order BFs may be used, depending on the data and physics of the problem. However, only the first-order and second-order BFs were used in this study. The coefficients β are estimated via the least-squares method during the two phases of the model, forward selection and backward deletion.

An example of how MARS uses piece-wise linear BFs to fit an expression to data is shown in Fig. 8. The corresponding MARS-based equation is given by,

$$y = 4.4668 + 1.1038 \times \boldsymbol{BF1} - 3.997 \times \boldsymbol{BF2} + 1.967 \times \boldsymbol{BF3} \quad (26)$$

where ***BF1*** = max(0, x - 16), ***BF2*** = max(0, 16 - x) and ***BF3*** = max(0, 25 – x). The three BFs delimit three intervals where different linear relationships are identified.

4.3. ARESLab Tool box used for MARS

In this study, the ARESLab toolbox (in MATLAB) is used to model the scour process with MARS (Jakabson, 2015). ARESLab is a multi-adaptive regression splines modeling algorithm. To use this toolbox, no specific assumption about the underlying functional relationship between the input variables and the output is required.

The foundational function, *Aresparams*, creates the structure of ARESLab configuration for use with other ARESlab functions. In *Aresparams*, the maximum number of BFs is initially set to 21 and the maximum interaction level of the input variables is set to 2. The forward selection process will continue until it reaches the predefined number of BFs. *Aresparams* initially utilizes the default setting of building a piece-wise cubic type model (i.e., cubic BFs). However, for simplicity, it can be set to a piece-wise linear type model (i.e., linear BFs). ARESlab uses the function *Aresbuild* to construct the model. Finally, MARS generates BFs and β coefficients.

Two combinations of data (dimensional and non-dimensional) were used as inputs in the MARS model. Our aim was to investigate which combination yields better results. In the first combination, dimensional variables including mean sediment diameter, (d_{50}), flow depth (y), average flow velocity (U), critical flow velocity (U_c), pile diameter (D), number of piles parallel to flow (m), number of piles perpendicular to flow (n), distance of the piles from each other

perpendicular to flow (S_n), and distance of piles from each other parallel to flow (S_m) were utilized to estimate d_{se} (see equation 1). In the second combination, non-dimensional variables including $\frac{U}{U_c}$, $\frac{U^2}{gD}$, $\frac{y}{D}$, $\frac{D}{d_{50}}$, $\frac{\rho UD}{\mu}$, $\frac{S_m}{D}$, $\frac{S_n}{D}$ and $\frac{m}{n}$ were used to estimate the dimensionless variable $\frac{dse}{D}$ (equation 2).

The initial input parameters of the ARESlab tool box are the default values in **Figure 9**. As seen in Table 7, "params" denotes parameters that are required by the ARESlab toolbox. These parameters are defined by the user in the following MATLAB command,

params = *Aresparams* (21, [], false, [], [], 2) (27)

where the value of 21 corresponds to the MaxFuncs. MaxFuncs is the maximum number of BFs in the forward phase of the model (before pruning in the backward phase). The recommended value for this parameter is about twice the expected number of BFs in the final model (Friedman, 1991). Note that the forward phase may not reach the specified maximum number of BFs. This can happen when the number of coefficients in the model exceeds the number of experimental data.

MaxFuncs can be computed automatically via the following formula,

maxFuncs = min (200, max (20, 2*d*)) +1 (28)

where *d* is the number of input variables (Milborrow, 2015).

```
params =

           maxFuncs: 21
                  c: 3
              cubic: 0
      cubicFastLevel: 2
    selfInteractions: 1
     maxInteractions: 2
           threshold: 1.0000e-04
               prune: 1
               fastK: Inf
            fastBeta: 0
               fastH: 1
          useMinSpan: -1
          useEndSpan: -1
       maxFinalFuncs: Inf
       endSpanAdjust: 1
       newVarPenalty: 0
```

Figure 9. Input parameters of ARESlab.

As shown in **Figure** 9, the second parameter (*c*) is the generalized cross validation (GCV) penalty per knot. This is also the second parameter in the *Aresparams* function. The literature suggests values in the range of 2 to 4 for *c* (Jekabsons, 2015). Larger values of *c* lead to fewer knots (i.e., the final model will be simpler). A value of 0 penalizes only terms, not knots. This can be useful with many data and low noise. The recommended (and default) value of *c* is 3 (Friedman, 1991), which is used in this study.

The third parameter in the *Aresparam* function (shown in **Figure 9** by "cubic") specifies whether to use the piecewise-cubic or piecewise-linear BFs. In this study, the piecewise-linear BFs were used instead of the default piecewise-cubic, and therefore the corresponding parameter in the *Aresparams* function is set to false.

The fourth parameter in the *Aresparams* function is "cubFastLevel" (**Figure 9.** Input parameters of ARESlab.). ARESlab implements three levels of piecewise cubic or linear modeling. In level 0, each candidate model is analyzed in both forward and backward (slow). For a faster

form of modeling, level 1 modelling only analyzes each candidate model in the backward phase (medium). In level 2, though modelling is done after both phases, it is only for the final iteration of the model, and is the fastest form of modeling. The default and recommended level is 2 (Jakabson, 2015).

The fifth parameter of the *Aresparams* function is the "selfInteractions". The selfInteractions is the maximum degree of self-interactions for any input variable. In ARESlab, it can be larger than 1 only for piecewise-linear BFs. Typically, the self-interactions are not allowed and the default value is 1, as shown in **Figure 9**.

The last parameter in the *Aresparams* function is "maxInteractions", which is the maximum degree of interactions between input variables. MaxInteractions of 1 means no interaction between the input variables. For maximal interactivity between the inputs "maxInteractions" should be set to *d*, "selfInteractions". This allows the modelling procedure to have the maximum freedom, leading to a complex structure. Typically, only a low degree of interaction is allowed, but higher degrees can be used when required. Herein, a typical value of 2 is used (**Figure 9**).

As shown in **Figure 9**, there are additional parameters that are used by ARESlab. These can be adjusted in the *Aresparams* function by adding other parameters in the function. The first of these parameters is "threshold". This is one of the stopping criteria for the forward phase. The larger the threshold, the simpler models are generated. The default value of threshold is set to 0.0001. For noise-free data , the threshold value may be lowered. "Prune" is the second of these parameters, which specifies whether to perform model pruning in the backward phase. The default value is set to 1, which allows to prune the model. The next parameter is the "fastK". This parameter determines the maximum number of BFs at each step of the forward phase (Friedman, 1993). Typical values for fastK are 20, 10, and 5. The default value is set to Inf or no Fast MARS.

With a lower fastK, building of the MARS model is faster, but its accuracy will be lower. A reasonable initial guess for fastK is 20 (Friedman, 1993). Friedman (1993) concluded that while changing the values of fastK and fastH can have a significant effect on the training time of MARS, its predictive performance is largely unaffected over a wide range of fastK and fastH values.

FastBeta is the artificial ageing factor in the Fast MARS algorithm (Friedman, 1993). The default value for fastBeta is 0 (no ageing factor) as is the case for this study, where Fast MARS algorithm is not used. As shown in **Figure 9**, the next parameter is fastH. FastH is an integer value for the Fast MARS algorithm (Friedman, 1993).

The next parameters are useMinSpan and useEndSpan. UseMinSpan is used to lower the local variance of the estimates. A minimum span is imposed that makes the technique resistant to runs of positive or negative error values between knots. This is done by jumping over a minSpan number of observations each time the next potential knot placement is requested (Friedman, 1991). UseMinSpan allows to disable the protection so that all input values are considered for knot placement in each dimension. Disabling minSpan may allow to create a model which is more responsive to local variations in the data. However, this can lead to an over fitted model. Setting the useMinSpan larger than 1 enables us to manually tune the value. In this study, the default and recommended value of -1 is used, which corresponds to the automatic mode. The useEndSpan parameter allows the user to lower the local variance of the estimates near the ends of the data intervals. A minimum span is imposed that makes the technique resistant to runs of positive or negative error values between extreme knot locations and corresponding ends of data intervals. This is done by not allowing to place a knot too near to the end of the data interval (Friedman, 1991). UseEndspan allows the user to disable (set to 0) the protection so that all observations are considered for knot placement in each dimension. Disabling endSpan may allow creating a model

which is more responsive to local variations in the data. However, this scan also lead to a model that is over fitted near the edges of the data. Setting the useMinSpan to larger than 1 enables us to manually tune the value. In this study, the default and recommended value of -1 is used, which corresponds to the automatic mode.

The user should also define maxFinalFuncs, endSpand Adjust and newVarPenalty. MaxFinalFuncs is the maximum number of BFs (including the intercept term) in the pruned model. This is used as an alternative to the maxFuncs parameter to enforce an upper bound on the final model size. In this study, the default value of Inf is chosen. EndSpanAdjust reduces probability of over fitting of interaction terms, which are supported by just a few observations in the boundaries of data intervals. Reasonable values for the EndSpanAdust range from 1 to 10, with the default value of 1. The third user defined parameter is newVarPenalty, which is the penalty for adding a new variable to a model in the forward phase. The higher the penalty is, the more reluctant the forward phase will be to add a new variable to the model (Friedman, 1991). Instead, it will try to use the variables, which were already in the model. This can be useful when some of the variables are highly collinear. As a result, the final model may be easier to interpret although the built model may be slightly less robust. Reasonable values for newVarPenaly typically vary from 0.01 to 0.2 (Milborrow, 2015). The default value is 0 or no penalty.

After the required parameters of MARS are specified (shown in Table 7), ARESlab begins the process of building the MARS model. Going through the forward and backward phases, it utilizes the user-defined parameters to develop the MARS model.

The ARESlab generates an ANOVA decomposition. Here is a quote from Friedman (1993), which helps us understand the ANOVA decomposition.

"The ANOVA decomposition is summarized by one row for each ANOVA function. The columns represent summary quantities for each one. The first column lists the function number. The second gives the standard deviation of the function. This gives one indication of its (relative) importance to the overall model and can be interpreted in a manner similar to a standardized regression coefficient in a linear model. The third column provides another indication of the importance of the correspond ANOVA function, by listing the GCV, score for a model with all of the basis functions corresponding to that particular ANOVA function removed. This can be used to judge whether this ANOVA function is making an important contribution to the model, or whether it just slightly helps to improve the global GCV score. The fourth column give s the number of basis functions comprising the ANOVA function while the fifth column provides an estimate of the additional number of linear degrees-of-freedom used by including it. The last column gives the particular predictor variables associated with the ANOVA function."

5. Results

5.1. Equilibrium scour depth estimates from the GEP model

The GEP model used both dimensional (Eq. 1) and non-dimensional (Eq. 2) data configurations. Our objective was to understand which configuration leads to better results.

5.1.1. Dimensional data

Dimensional input ($D, y, U, U_c, d_{50}, S_m, S_n, n,$ and m) and output (d_{se}) data were used to train the GEP model. After 500,000 generations, the fitness function converged to a value of 0.0187 (m) and no significant changes were observed in it. Hence, training of GEP was terminated after 500,000 generations.

The final expression tree (ET) from the GEP model is indicated in **Figure 10**. It includes 4 sub-ETs linked by the addition operator (+). Each of the sub-ETs contains a number of the specific functions in **Table 9**, independent variables ($D, y, U, U_c, d_{50}, S_m, S_n, n,$ and m), and constant parameters in **Table 8**.

Table 8. Parameters of the GEP model.

Number of chromosomes	30
Head size	8
Number of genes	3
Linking function	Addition
Fitness function	RMSE
Mutation rate	0.044
Inversion rate	0.1
One-point recombination rate	0.3
Two-point recombination rate	0.3
Gene recombination rate	0.1
Insertion sequences transposition rate	0.1
Root insertion sequence transposition rate	0.1
Gene transposition rate	0.1
Function set	$+, -, \times, /, \sqrt{}, e^x, Sin, Cos, Tan, Tanh, Arctan, Ln$

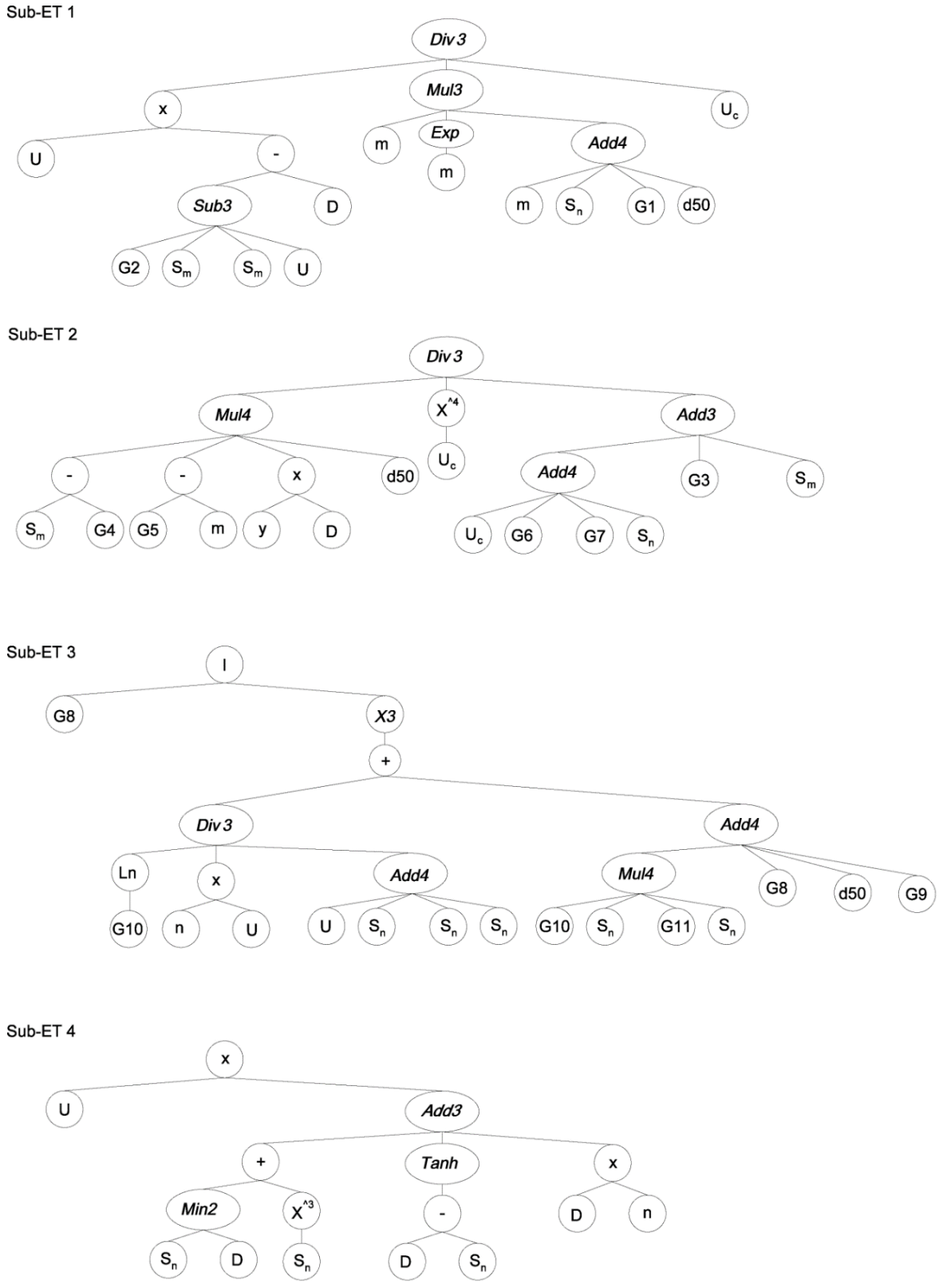

Figure 10. Expression tree (ET) from the GEP model.

The GEP-based equation for prediction of equilibrium scour depth (d_{se}), Eq. (1), in terms of $D, y, U, U_c, d_{50}, S_m, S_n, n,$ and m can be obtained from the expression tree (**Figure 10**) and is given by,

$$d_{se} = \frac{U[(G_2 - 2S_m - U) - D]}{me^m\,(m + S_n + G_1 + d_{50})U_c} + \frac{(S_m - G_4)(G_5 - m)yDd_{50}}{{U_c}^4\,(U_c + G_6 + G_7 + G_3 + S_n + S_m)} + \frac{G_8}{[\mathrm{Ln}(G_{10})/(nU(U + 3S_n)) + G_{10}G_{11}{S_n}^2 + G_8 + G_9 + d_{50}]^3} + U[\min(S_n, D) + {S_n}^3 + \tanh(D - S_n) + nD] \quad (29)$$

Values of various constant parameters in equation (29) are listed in **Table 9**. Eq. (29) implies that a complicated nonlinear formula is required to accurately predict equilibrium scour depth. Derivation of such an equation is very hard from conventional regression-based approaches.

Table 9. Magnitudes of constant parameters in **Figure 10** and equation 29.

Parameter	Value
G_1	-4.420
G_2	0.047
G_3	0.968
G_4	9.135
G_5	-1.472
G_6	6.278
G_7	-5.487
G_8	-6.987
G_9	1.965
G_{10}	0.617
G_{11}	11.002

A comparison of the predicted and observed equilibrium scour depth values is shown in **Figure 11** for both training and testing phases. As shown, the equilibrium scour depth estimates agree well with the observed values in training and testing. The outcomes also indicate that GEP slightly outperforms in training (with MAE, RMSE and R^2 0.0130 m, 0.0187 m, and 0.911) compared to testing (with MAE, RMSE, and R^2 of 0.0162 m, 0.0254 m, and 0.879). Overall, the results indicate that the predicted scour depth values are close to the measurements, suggesting that the derived equation from GEP can be used to reliably estimate d_{se} from $D, y, U, U_c, d_{50}, S_m, S_n, n,$ and m.

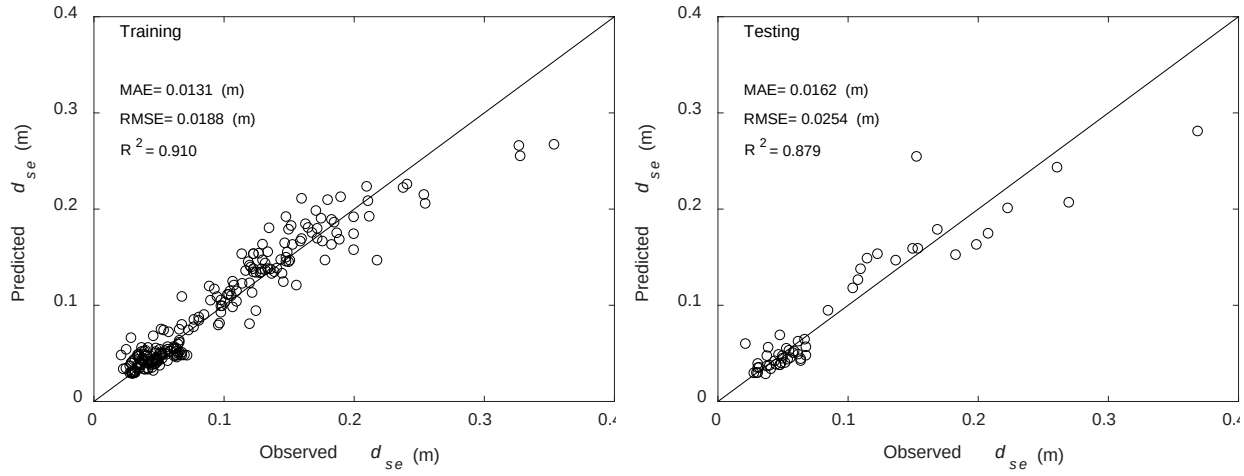

Figure 11. Predicted equilibrium scour depth (d_{se}) from GEP versus observations for dimensional data set (Eq. 1).

5.1.2. Non-dimensional data

The non-dimensional form of data (Eq. 2) was also used in the GEP model to estimate equilibrium scour depth (**Figure *12***). This was done to evaluate which of the data configurations (dimensional or non-dimensional) could generate better results. In the training step, the MAE and

RMSE of scour depth estimates were respectively 0.0162 m and 0.0234 m, which are 24.6% and 25.1% larger than those of the dimensional dataset. Similarly, in the testing step, the MAE and RMSE increase by 23% and 14% when non-dimensional data is used instead of dimensional. These results showed that the GEP model performed better when trained with the dimensional data (Eq. 1) than the non-dimensional data (Eq. 2). This suggests that utilizing constitutive raw variables instead of their groupings leads to more accurate results due to the increased flexibility in fitting achieved in that way.

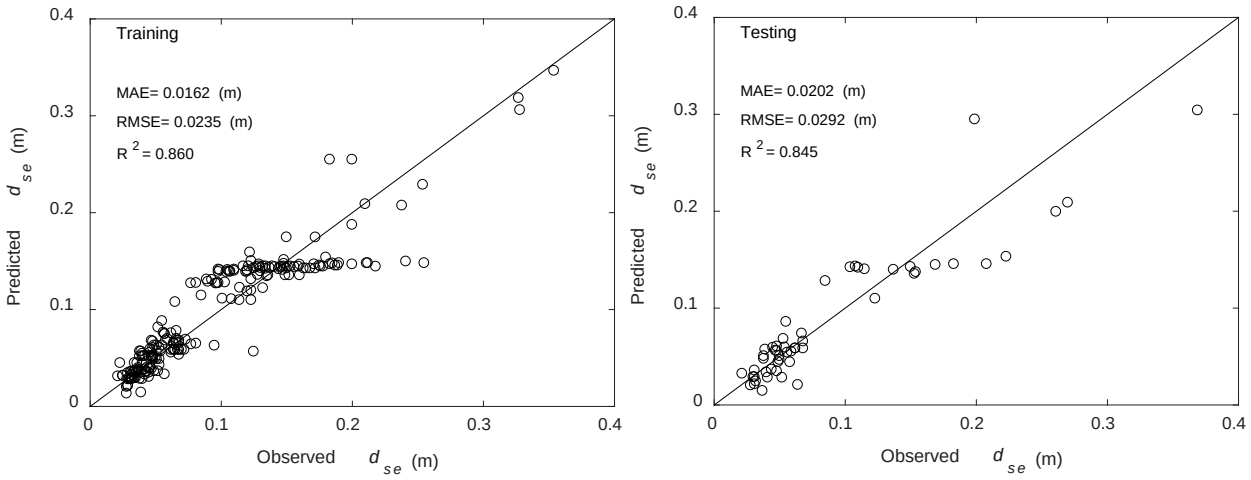

Figure 12. Predicted equilibrium scour depth (d_{se}) from GEP versus observations for non-dimensional data set (Eq. 2).

5.2. Equilibrium scour depth estimates from the MARS model

Both dimensional (Eq. 1) and non-dimensional (Eq. 2) data configurations were used in MARS. Our aim was to find which configuration yielded better results

5.2.1. Dimensional Data

The number of basis functions in the forward step (*nb*) and degree of interaction (*deg*) influence performance of MARS. In this study, *nb* and *deg* were varied in the range of 1-25 and 1-2, respectively. Finally, *nb* and *deg* values that led to the best equilibrium scour depth estimates were chosen. The MARS model with *deg* of 1 (i.e., no interaction effect) yielded a simple expression for the estimation of d_{se}, but it performance was not as good as the model with *deg* of 2. Hence, *deg* of 2 was used in this study. **Figure *13*** shows variations of RMSE versus the number of basis functions for the training step.

As indicated, the RMSE of d_{se} estimates decrease as the number of basis functions increases, ultimately reaching an asymptotic value of 0.0110 (m) for *nb* of 26. Based on **Figure *13***, *nb* is set to 26 because a higher *nb* value does not improve performance of the MARS model and only increases its complexity.

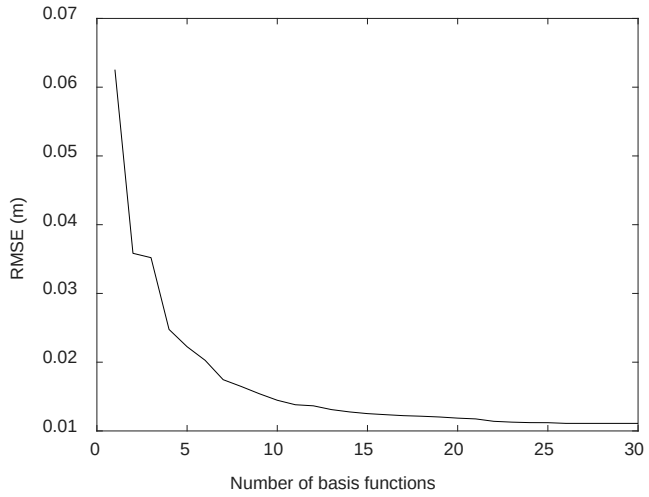

Figure 13. Variation of RMSE versus number of basis functions in training step

The computed coefficients (β_i) and basis functions ($B_i(x)$) from the MARS model are listed in **Table 10**. They can be substituted in the general form of MARS (Eq. 25) to generate an equation for the estimation of the equilibrium scour depth in terms of $D, y, U, U_c, d_{50}, S_m, S_n, n,$ and m. As

indicated in this table, the variables D, n, and S_n emerge in the MARS-based equation both individually and interactively. In contrast, U, U_c, y, m, and S_m appear only as interactive variables.

Figure *14* shows the equilibrium scour depth estimates from MARS versus observations. Most of the data points fall around the 1:1 line, implying that the MARS model can accurately predict d_{se}. The results from MARS had a small MAE of 0.0079 m and RMSE of 0.0110 m, and high R^2 of 0.969 in the training step. In the testing phase, the MAE = 0.0120 m and RMSE = 0.0174 m were larger and R^2 = 0.952 was lower compared to the training step. Overall, the results showed that MARS has performed well in estimating the equilibrium scour depth.

Table 10. Basis functions and coefficients of the MARS model.

Basis functions ($B_i(x)$)	Coefficients (β_i)
Intercept	0.2054
$(0.05 - D)+$	−5.4888
$(n - 3)+$	0.0285
$(3 - n)+$	0.0361
$(S_n - 0.0184)+ \times (U - 0.31)+$	− 8.9735
$(S_n - 0.0184)+ \times (0.31 - U)+$	− 14.2360
$(S_n - 0.0184)+ \times (y - 0.24)$	1.3787
$(S_n - 0.0184)+ \times (0.24 - y)$	3.0331
$(3 - n)+ \times (D - 0.024)+$	−1.1594
$(S_n - 0.15)+$	17.9990
$(3 - n)+ \times (S_n - 0.06)+$	0.8013
$(3 - n)+ \times (0.06 - S_n)+$	− 0.9569
$(S_n - 0.0184)+ \times (U_c - 0.32)+$	− 0.2078
$(S_n - 0.0184)+ \times (0.32 - U_c)+$	17.8451
$(0.15 - S_n)+ \times (m - 5)+$	0.3283
$(0.15 - S_n)+ \times (5 - m)+$	−0.0099
$(S_n - 0.15)+ \times (d_{50} - 0.8)+$	−86.2240
$(S_n - 0.15)+ \times (0.8 - d_{50})+$	− 103.0101
$(0.0184 - S_n)+ \times (y - 0.2)+$	− 62.3371
$(0.0184 - S_n)+ \times (0.2 - y)+$	9.8549
$(0.15 - S_n)+ \times (D - 0.028)+$	17.1142
$(0.15 - S_n)+ \times (0.028 - D)+$	22.9282
$(S_n - 0.0184)+ \times (n - 3)+$	− 0.2319
$(S_n - 0.0184)+ \times (3 - n)+$	−0.7851
$(3 - n)+ \times (0.068 - y)+$	−0.2423
$(S_n - 0.0184)+ \times (S_m - 0.125)+$	−0.7108
$(S_n - 0.0184)+ \times (0.125 - S_m)+$	− 0.8789

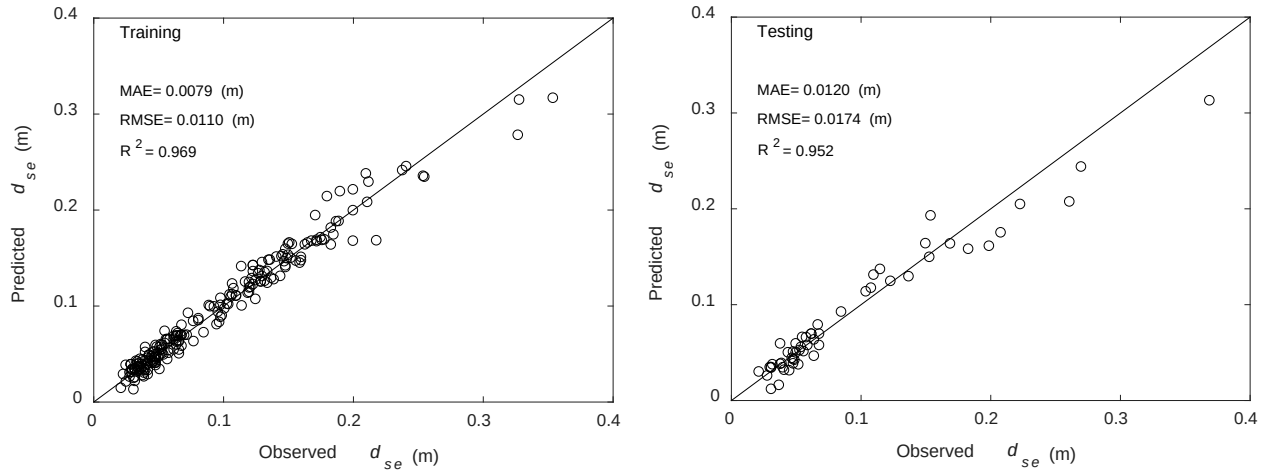

Figure 14. Predicted equilibrium scour depth (d_{se}) from MARS versus observations for dimensional data set (Eq. 1).

5.2.2. Non-dimensional data

Similar to the GEP model (Section 5.1.2), non-dimensional data were used to train MARS. The equilibrium scour depth estimations are shown versus observations in **Figure *15***. The model performed well in predicting the equilibrium scour depth in both training (MAE = 0.0102 m, RMSE = 0.0155 m, and R^2 = 0.939) and testing (MAE = 0.0144 m, RMSE = 0.0191 m, and R^2 = 0.935) stages. The results also showed that the MARS model generated better results when analyzed with dimensional inputs (Eq. 1) rather than the non-dimensional inputs (Eq. 2). This implies that using constitutive raw variables in lieu of their groupings yields more promising results because of the better flexibility in fitting a relationship between inputs and output (Bateni et al., 2007).

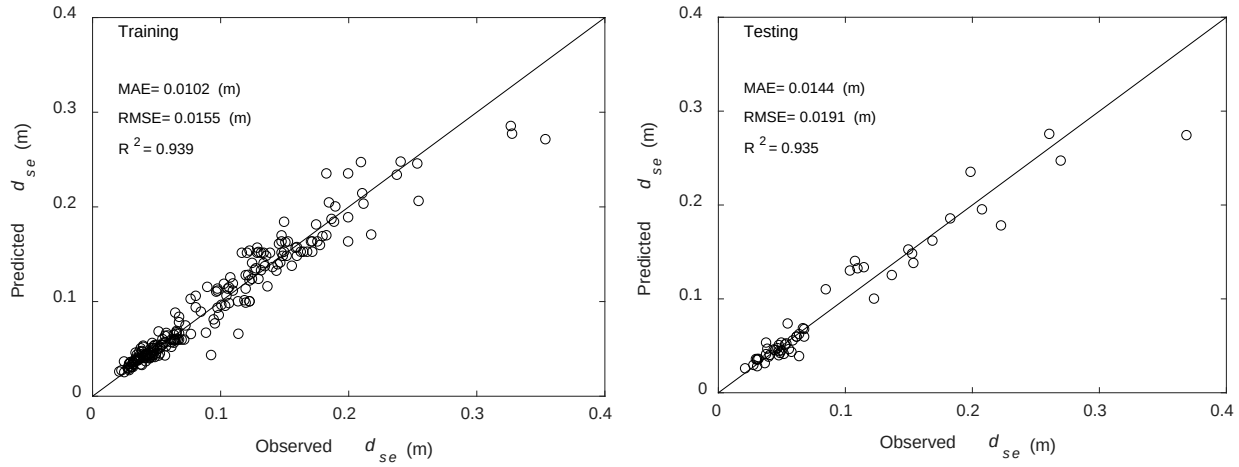

Figure 15. Predicted equilibrium scour depth (d_{se}) from MARS versus observations for non-dimensional data set (Eq. 2).

5.3. Comparison of equilibrium scour depth estimates from MARS and GEP with those of existing equations

Figure ***16*** compares the equilibrium scour depth estimates from MARS with those of the five existing equations. The results from GEP are not shown in **Figure *16*** to keep it readable and not too congested. As shown, the existing equations generally underestimate the equilibrium scour depth, while MARS provides improved estimates of equilibrium scour depth and its results fall mainly around the 1:1 line. As indicated in **Table *11***, the proposed models (i.e., MARS and GEP) outperform the existing studies. For the best available study (Sheppard et al., 2013), the MAE, RMSE, and R^2 are respectively 0.0197 m, 0.0297 m, and 0.836, compared to 0.0120 m, 0.0174 m and 0.952 for the MARS model. MARS reduces RMSE of scour depth estimates by 57%, 55%, 41%, 56%, and 49% compared to Richardson et al. (2001), Beheshti et al. (2012), Sheppard et al. (2013), and equations 13 and 14 in Ghaemi et al. (2013), respectively. The results in **Table *11*** also show that MARS yields better results than GEP. MAE and RMSE from MARS are 26% and 31% less than those from GEP. Both GEP and MARS models can create explicit equations for

estimation of equilibrium scour depth. Overall, the results of this study suggest that MARS and GEP are viable alternative techniques to the existing equations.

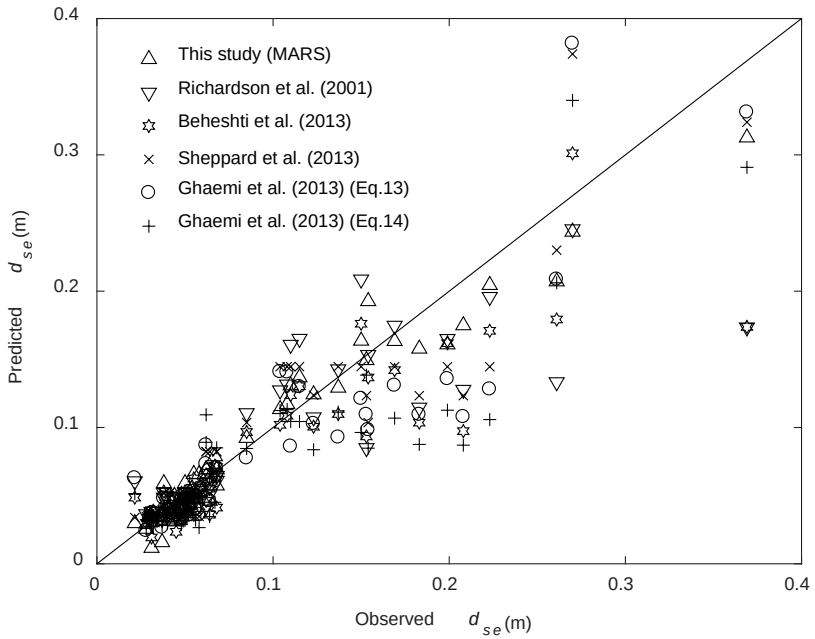

Figure 16. Comparison of equilibrium scour depth measurements and estimations using different approaches.

Table 11. Statistical metrics of different approaches to estimate scour depth.

Different approaches	MAE (m)	RMSE(m)	Correlation coefficient (R^2)
This study (MARS)	**0.0120**	**0.0174**	**0.952**
This study (GEP)	**0.0162**	**0.0254**	**0.879**
Richardson et al. (2001)	0.0209	0.0401	0.716
Beheshti et al (2013)	0.0208	0.0386	0.772
Sheppard et al. (2013)	0.0197	0.0297	0.836
Ghaemi et al. (2013)	0.0263	0.0394	0.768
Ghaemi et al. (2013)	0.0220	0.0341	0.800

5.4 Sensitivity Analysis

The generated equation from MARS (i.e., the best available equation) was used to conduct the sensitivity analysis. This analysis was performed to find the relative importance of each of the input variables ($D, y, U, U_c, d_{50}, S_m, S_n, n,$ and m) on the equilibrium scour depth. In each sensitivity test, only one of the input variables was changed at a constant rate, and its influence on d_{se} was determined. Inputs were varied at the constant rates of 10%, 30%, and 50%. The sensitivity of equilibrium scour depth (d_{se}) to changes in each input variable is computed via:

$$d_{se}\ (\%) = \frac{1}{N}\sum_{i=1}^{N}\left(\frac{\%\ \text{Change in } d_{se}}{\%\ \text{Change in the input variable}}\right) \times 100 \quad (30)$$

where N = 54 is number of testing data points used in this study.

Figure 17a, **b**, and **c** show the sensitivity of d_{se} to 10%, 30%, and 50% changes in each input variable, respectively. As indicated, D has the most significant impact on the equilibrium scour

depth. A similar result was reported by Zounement-Kermani et al. (2009). They also found that U_c and U have a high influence on d_{se}, which is consistent with the results of our sensitivity analysis.

Ataie-Ashtiani and Beheshti (2006) proposed the following equation for the estimation of equilibrium scour depth

$$d_{se} = 2.22\, k_1 k_2 k_3 k_4\, \frac{(D_{proj}\, K_G\, K_m)^{0.7653}\; m^{0.0396}}{n^{0.5225}\; G^{0.1153}} \left(\frac{y\, U}{U_c}\right)^{0.35} \tag{31}$$

where $k_1, k_2, k_3,$ and k_4 are the correction factors for pier nose shape, angle of attack, channel bed condition, and bed armoring, respectively. D_{proj} is the sum of the non-overlapping projected widths of piles, K_G is the coefficient for pile spacing, K_m is the coefficient for the number of aligned rows, and G is the pile spacing. According to Eq. (30), d_{se} increases with growth of m, U, y and D, and decreases with increase of U_c and n. Analogously, Figure 17 indicates that d_{se} is positively correlated with y, U, D and m, while it is negatively correlated with U_c and n.

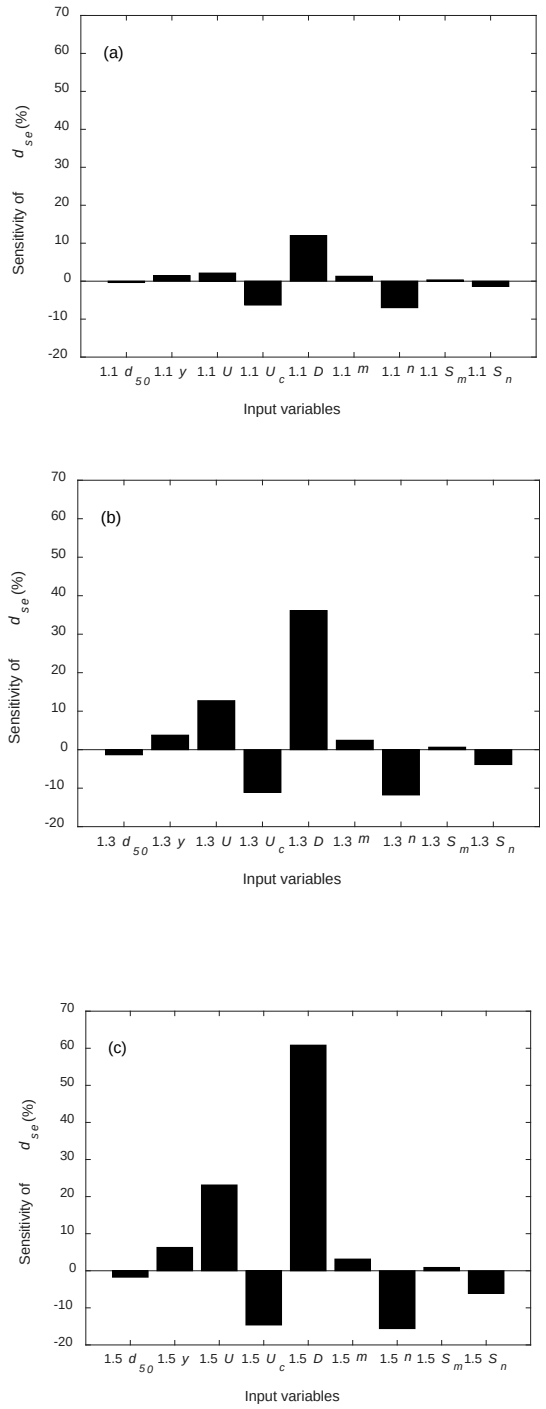

Figure 17. Sensitivity of equilibrium scour depth to 10% (**a**), 30% (**b**), and 50% (**c**) variations in each input variable.

6. Conclusion

Genetic Expression Programming (GEP) and Multivariate Adaptive Regression Splines (MARS) approaches were used to estimate equilibrium scour depth (d_{se}) around pile groups. Two configurations of data (dimensional and non-dimensional) were used in the GEP and MARS models. The results indicated that GEP and MARS can accurately estimate d_{se}. Also, both models yielded better d_{se} estimates with the dimensional data. MARS outperformed GEP. The equilibrium scour depth estimates by GEP and MARS have a root-mean-square-error (RMSE) of 0.0254 m and 0.018 m, respectively. Corresponding mean-absolute-error (MAE) values are 0.0162 m and 0.0131 m. Overall, the results indicate that MARS and GEP are effective and reliable methods for estimating equilibrium scour depth.

Performance of MARS and GEP was compared with four existing studies, namely Richardson et al. (2001), Beheshti et al (2013), Sheppard et al. (2013), and Ghaemi et al. (2013). The results illustrated that GEP and MARS can estimate equilibrium scour depth more accurately. MARS reduced the MAE (RMSE) by 43% (57%), 42% (55%), 39% (41%), 54% (56%), and 45% (49%) compared to Richardson et al. (2001), Beheshti et al (2013), Sheppard et al. (2013), and equations 13 and 14 in Ghaem et al. (2013). A similar reduction was seen in MAE and RMSE by using GEP instead of existing equations. In general, the results showed that GEP and MARS perform well and thus can be used to accurately estimate equilibrium scour depth.

Sensitivity analysis was conducted to assess the influence of each input variable on the equilibrium scour depth. It was found that pile diameter has the most significant impact on the equilibrium scour depth. Also, the flow velocity and critical flow velocity have a substantial effect on d_{se}. Overall, d_{se} is positively correlated with flow depth and velocity, pile diameter, number of piles inline with the flow, and the spacing between piles inline with the flow, while it is inversely

related to mean grain diameter, critical flow velocity, number of piles normal to the flow, and spacing between piles normal to the flow.

References:

Adamowski, J., Chan, H. F., Prasher, S. O., sharda, V. N. (2012), *Comparison of Multivariate Regression Splines with Coupled Wavelet Transform Artificial Neural Networks for Runoff Forecasting in Himalayan Micro-Watersheds with Limited Data*, Journal of Hydroinformatics, 14(3), 731-744.

Ahmand, M., (1953), *Experiments on Design and Behavior of Spur Dikes*. Proceedings of the International Association of Hydraulic Research, American Society of Civil Engineers Joint Meeting, Untiersity of Minnesota, August.

Amini A, Melville B, Ali T, Ghazali, A., 2012. *Clear-water local scour around pile groups in shallow-water flow*. J Hydraul Eng 138(2):177–185.

Anich, Mike (2017), *The Day the Bridge Fell*. The Leader-Herald, April 9, 2017.

Ataie-Ashtiani, B. and Beheshti, A.A. (2006). *Experimental investigation of clear-water local scour at pile groups*. Journal of Hydraulic Engineering, 132, 1100–1104.

Ataie-Ashtiani, B., Baratian-Ghorghi, Z., and Beheshti, A. A (2010). *Experimental Investigation of Clear-Water Local Scour of Compound Piers*. Journal f Hydraulic Engineering, June 2010, 343-351.

Azamathulla, H. Md (2012). *Gene-Expression Programming to Predict Scour at a Bridge Abutment*. Journal of Hydroinformatic, 14.2, 324-331.

Azamathulla, H. Md. (2012). *Gene Expression Programming for Prediction of Scour Depth Downstream of Sill, Journal of Hydrology*, 460-461, 156-159.

Azamathulla, H. Md., Ahmad, Z. (2012). *Gene-Expression Programming for Transverse Mixing Coefficient*. Journal of Hydrology 434-435C, 142-148.

Azamathulla, H.Md and Wu, F. (2011). *Support Vector Machine Approach for Longitudinal Dispersion Coefficients in Streams*, Applied Software Computing 11(2), 2902 – 2905.

Azamathulla, H. Md., and Jarret, R. D., 2013. *Use of gene-expression programming to estimate manning's roughness coefficient for high gradient streams*, Water Resources Management, 27(3), 715-729.

Bateni S.M., S.M. Borghei, and D.S. Jeng (2007a). *Neural Network and Neuro-Fuzzy Assessments for Scour Depth Around Bridge Pier*s. ScienceDirect, Engineering Applications of Artificial Intelligence 20, 401-414.

Bateni, S. M., Jeng, D. S., and Melville, B. W. (2007b), *Bayesian Neural Networks for Prediction of Equilibrium and Time-Dependent Scour Depth around Bridge Piers*, Advances in Engineering Software, 38, 102-111.

Beheshti, A., Ataie-Ashtiani, B., Khanjani, M., 2013. *Discussion of clear-water local scour around pile groups in shallow-water flow* by Ata Amini, Bruce W Melville, Thamer M Ali, Abdul H Ghazali. J Hydraul Eng, 139(6), 679–680

Cheng, M. Y., and Cao, M. T. (2014), *Evolutionary Multivariate Adaptive Regression Splines for Estimating Shear Strength in Reinforced-Concrete deep beams*, Engineering Applications of Artificial Intelligence.

Choi, S. U., and Jung, S. H. (2006), *Prediction of Local Scour Around Bridge Piers Using Artificial Neural Networks*, Journal of the American Water Resources Association, 42(2), 487-494.

Choi, S U., Choi, B., and Choi, S. (2015), *Improving Predictions Made by ANN Model Using Data Quality Assessment: an Application to Local Scour Around Bridge Piers*, Journal of Hydroinformatics, 17(6), 977-989.

Coleman, S. E. (2005). *Clearwater local scour at complex piers*. Journal of Hydraulic Engineering, 131(4), 330-334.

Dey, S & Barbhuya, A. K. (2004a). *Clear Water Scour at Abutments*. Proc. Inst. Civil Engineering Water. Management. 157, 77-97.

Dey, S. & Barbhuya, A. K. (2004b). *Clear Water Scour at Abutments in Thinly Armored Beds*. Journal of Hydraulic Engineering. 130 (7), 622-634.

Emamgolizadeh, S., Bateni, S. M., Shahsavani, D., Ashrafi, T., and Ghorbani, H. (2015), *Estimation of Soil Cation Exchange Capacity Using Genetic Expression Programming (GEP) and Multivariate Regression Splines (MARS)*, Journal of Hydrology, 529(3), 1590-1600

Etemad-Shahidi, A., Yasa, R and Kazeminezhad, MK. (2011). *Prediction of wave-induced scour depth under submarine pipelines using machine learning approach*." Applied Ocean Research, 33, 54-59.

Ettema, R., Melville, B.W. and Barkdoll, B. (1998). *Scale effect in pier-scour experiments. Journal of Hydraulic Engineering*. 124, 639–642

Ferraro, D., Ali, T., Gaudio, R., and Cardoso, A.H. (2013). *Effects of Pile Cap Thickness on the Maximum Scour Depth at a Complex Pier*, Journal of Hydraulic Engineering, Vol. 139, Issue 5 (May 2013)

Ferreira, C. (2001a). *Gene Expression Programming: A New Adaptive Algorithm for Solving Problems. Complex Systems 12 (2), 87 -129.*

Ferreira, C. (2001b). *Gene Expression Programming in Problem Solving*. In Proc. 6th Online World Converence on Soft Computing in Industrial Applications. Invited tutorial, pp. 10 - 24.

Friedman, J.H. (1991). *Multivariate Adaptive Regression Splines*. The annals of statistics vol. 19, No. 1, 1-141.

Friedman, J.H. (1993). *Fast MARS, Department of Statistics, Stanford University, Tech. Report LCSS110*. The annals of statistics vol. 19, No. 1, 1-141.

Gandomi, A. H. and Alavi, A. H. (2011), *Multi-stage Genetic Programming: A New Strategy to Nonlinear System Modeling*, Inf. Sci. 181(23), 5227-5239.

Ghaemi, N., Etemad-Shahidi, A., Ataie-Ashtiani, B., 2013. *Estimation of current-induced pile groups scour using a rule based method*. J. Hydroinformatics, 15(2), 516–528.

Grimaldi, C. and Cardoso, A. H. (2010). *Methods for Local Scour Depth Estimation at Complex Bridge Piers*. Hydraulic Structures Division, Lombardi SA Engineering Limited, Minusio, Swtizerland.

Guven, A., and Aytek, A. (2009), *New Approaches for Stage-Discharge Relationship: Gene-Expression Programming*, Journal of Hydrologic Engineering, 14(8), 812-820.

Guven, A., and Azamathulla, H. Md. (2012), *Gene-Expression Programming for Flip-Bucket Spillway Scour*, Water Science and Technology, 65(11), 1982-1987.

Guven, A., Gunal, M. (2008), *Genetic Programming Approach for Prediction of Local Scour Downstream of Hydraulic Structures*, Journal of Irrigation Drainage Engineering, 134 (2), 241-249.

Hill, K. (2013), *Why Most Bridges Fail*, Scientific American Blog Network, May 24, 2013

Jakabsons G. (2015). *ARESLab: Adpative Regression Splines toolbox for Matlab/Octave*, available at http://www.cs.rtu.lv/jekabsons

Kaya, A. (2010), *Artificial Neural Network Study of Observed Pattern of Scour Depth Around Bridge Piers*, Computers and Geotechnics, 37(3), 413-418.

Kisi, O., Shiri, J. (2012). *River suspended sediment estimation by climatic variables implication: Comparative Study Among Soft Computing Techniques*. Computers and Geosciences, June 2012, Vol.43, pp.73-82.

Koza, J. R. (1999). *Genetic Programming: on the Programming of computers by Means of Natural Selection*. MIT Press, Cambridge, MA.

Kothyari, U.C., Grade, R. J., and Ranga Raju, K.G. (1992). *Temporal Variation of Scour Around circular Bridge Piers.* Journal of Hydraulic Engineering 119 (8), 1091-1106.

Lanca, R., Fael, C., Maia, R., Pego, J., and Cardoso, A. (2013) Clear-water scour at Pile Groups. Journal of Hydraulic Engineering, October 2013, 1089-1098

Martin-Vide, J.P., Hidalgo C., and Bateman, A (1998). *Local Scour at Pile Bridge Foundations*. Journal of Hydraulic Engineering, Vol. 124 (4), April.

Melville, B. W., Chew, Y. M. (1999), *Time Scale for Local Scour Depth at Bridge Piers*, Journal of Hydraulic Engineering , 125(1), 59-65.

Milborrow, S., (2015). *Earth: Muultivariate Adaptive Regression Spline Models* (derived from code by T. Hastie and R. Tibshriani), R package available at http://cran.rproject.org/src/contrib/Descriptions/earth.html

Moreno, M., Maia, R. and Couto, L. (2015). *Effects of relative column width and pile-cap elevation on local scour depth around complex piers*. Journal of Hydraulic Engineering

Mueller, D.S. and J.S. Jones, (1999), *Evaluation of Recent Field and Laboratory Research on Scour at Bridge Piers in Coarse Bed Materials,* ASCE Compendium Stream Stability and Scour at Highway Bridges, Richardson and Lagasse (eds.), Reston, VA.

Muhammad, N. A. (2003*). Top Ten Software Used in Civil Engineering.* http://civilvalley.bogspot.com/2013/09/top-ten-software-used-in-civil.html

Richardson, E.V. and Davis, S.R. (2001). *Evaluating scour at bridges*. Hydraulic 9 Engineering Circular No. 18 (HEC-18), Rep. No. FHWA NHI 01-001, Federal Highway 10 Administration, Washington, D.C.

Samui, P., Das, S., Kim, D. (2011), Uplift Capacity of Suctino Caisson in Clay Using Multivariate Adaptive Regression Spline, Ocean Engineering, 38, 2123-2127.

Samui, P. (2011). *Determination of Ultimate Capacity of Driven Piles in Cohesionless Soil: A Multivariate Adaptive Regression Spline Approach,* Introductional Journal for Numerical and Analytical Methods in Geomechanics, 36(11), 1444-1439.

Sattar, A.M. (2014). *Gene Expression Models for Prediction of Dam Breach Parameters*. Journal of Hydroinformation. IWA (in press). http://dx.doi.org/10.2166/hydro.2013.084,<http://www.iwaponline.com/jh/up/jh2013084.htm>

Sheppard, D., Melville, B., and Demir, H., 2013. "*Evaluation of existing equations for local scour at bridge piers*." Journal of Hydraulic Engineering, Vol. 140, No. 1, pp. 14-23, DOI: 10.1061/(ASCE) HY.1943-7900.0000800.

Shiri, J., Marti, P., and Singh, V. P. (2012), *Evaluation of Gene Expression Programming Approaches for Estimating Daily Evaporation Through Spatial and Temporal Data Scanning*, 28(3), 1215-1225.

Toth, E., and Brandiarte, L. (2011*), Prediction of Local Scour Depth at Bridge Piers Under Clear-Water and Live-Bed Conditions: Comparison of Literature Formulae and Artificial Neural Networks*, Journal of Hydroinformatics, 13(4), 812-824. Doi: 10.2166/hydro.2011.065

Toth, E. (2015), *Asymmetric Error Functions for Reducing the Underestimation of Local Scour Around Bridge Piers: Application to Neural Networks Models, Journal of Hydraulic Engineering*, 141(7), doi: 10.1061/(ASCE)HY.1943-7900.0000981

Read More: http://ascelibrary.org/doi/abs/10.1061/(ASCE)HY.1943-7900.0000981

US Dot, (1993), *Evaluating Scour at Bridges*, Hydraulic Engineering Circular No. 18. FHWA-IP-90-017, Federation of Hwy. Administration, US Department of Transportation, McLean, VA.

Vasquez, J. (2004). *Pile Scour*. PepeVasquez.com. January 15, 2004

Wardhana, K. and Hadipriono, F. (2003). *Analaysis of Recent Bridge Failure in the United States*. Journal of Performance of Constructed Facilities, 10. 1061/(ASCE)0887-3828(2003), 17:3(144), 144-150.

Zakaria, N. A., Azamathulla, H. Md, Chang, C. K., and Chani, A. A. (2010), Gene Expression Programming for Total Bed Material Load Estimation – A Case Study, Sci. Total. Environ. 408, 5078-5085.

Zhang, W.G. and Goh, A.T.C. (2013). *Multivariate A.* Geotechnique 53, No. 1, 11-25.